united nations
educational, scientific
and cultural
organization

international atomic
energy agency

the
abdus salam
international centre for theoretical physics

SMR/1083 - 4

SUMMER COLLOQUIUM ON THE PHYSICS OF WEATHER & CLIMATE
"THE EFFECT OF TOPOGRAPHY ON THE ATMOSPHERIC CIRCULATION"
8 - 19 JUNE 1998

"Numerical Methods: the Arakawa Approach, Horizontal Grid, Global & Limited-Area Modeling"

F. MESINGER
NOAA, Science Center
Camp Springs, MD
USA

Numerical methods: The Arakawa approach, horizontal grid, global and limited-area modeling

Fedor Mesinger

NOAA Environmental Modeling Center/UCAR Visiting Scientist Program
Camp Springs, MD

15 May 1998

Submitted to "General Circulation Model Development: Past, Present and Future"
Proceedings of a Symposium in honor of Professor Akio Arakawa
Edited by David Randall
Academic Press

Abstract

The Arakawa approach in numerical methods is summarized. While maintenance of the difference analogs of chosen integral constraints of the continuous atmosphere is the hallmark of the approach, emphases is also placed on reproducing numerous other properties of physical importance of the fluid dynamical system addressed. Underlying the approach is the determination to understand the reason of a numerical problem and address its cause as opposed to using artificial diffusion to alleviate its consequences and lose some of the real information in the process.

Issues of the choice of horizontal grid are reviewed, as an illustration of the diversity of considerations made. A number of recent ideas are summarized. Included are topics of the Arakawa C and the B/E grid-like hexagonal grids, and of a family of square B/E grid gravity-inertia wave schemes with "C-grid-like" propagation of gravity waves.

While conceptually the Arakawa approach was expected to be the most rewarding in climate integrations, it may be that the limited area Eta weather prediction model has provided the strongest indication yet of the benefits the approach brings. The numbers behind this statement are presented.

Several recent results and issues in model design are summarized or commented upon, having to do with the pole problem, the validity of the limited-area approach, and the resolution vs domain size trade-off.

Recent progress and state-of the-art in modeling skill are summarized. Concluding remarks are made on areas of active research in numerical schemes, and on possible future trends.

---

1. Introduction: The Arakawa approach in numerical methods

It is perhaps a remarkable characteristic of atmospheric numerical modeling that in spite of the steady progress during the past more than four decades the diversity of points of view on what are the most promising principles to follow shows little sign of diminishing. Within these points of view, I find it fitting to refer to the Arakawa approach in numerical modeling as the one in which attention is focused on the realism of the physical properties of the discrete system within given computational resources. With the Arakawa approach, one is thus not relying on these properties to automatically become satisfactory as the resolution is increasing, as a result of

the observation of basic requirements of the computational mathematics. Instead, one is striving to achieve properties deemed desirable with the resolution at hand. This is achieved by consideration of the physical properties of the finite difference analog of the continuous equations.

With this formulation, there is clearly some room left for searching as to what exactly are the physical properties to which attention is best paid, and to what should be the priorities among various possibilities. The famous Arakawa (1966) horizontal advection scheme, and subsequent numerous conservation considerations as discussed in Arakawa and Lamb (1977, hereafter AL) for example have established the maintenance of the difference analogs of chosen integral constraints of the continuous atmosphere as the hallmark of the approach. Yet, more generally, emphasis was placed by Arakawa and by others on reproducing numerous other properties of physical importance of the fluid dynamical system addressed. Dispersion and phase speed properties, avoidance of computational modes, and avoidance of false instabilities are the typical examples, as succinctly summarized recently in Section 7 of a recent review paper by Arakawa (1997); or, more extensively, in Arakawa (1988).

In striving to achieve the goals of this type, no advantage tends to be obtained from increasing the order of the accuracy of the scheme. For example, as gently stated by Arakawa (1997) in summarizing the problem of the computational mode, "The concept of the order of accuracy ... based on the Taylor expansion ... is not relevant for the existence or non-existence of a computational mode". Similarly, Mesinger (1982; see also Mesinger and Janjic, 1985) demonstrated that an increase in resolution which entails an increase in the formal Taylor series accuracy does not necessarily help in achieving a physically desirable result and can even result in an increase of the actual error.

Underlying the Arakawa approach is the determination to understand the reason of a numerical problem and address its cause as opposed to using artificial diffusion or filtering to alleviate its consequences and lose some of the real information in the process. Yet, very different views are not hard to find among leading atmospheric modelers. For example, in a recent paper one reads that "such short waves [wavelengths less than $4\Delta x$] are inadequately resolved on a computation grid and even in the linearized equations are poorly represented in terms of amplitude and/or phase. For these reasons, and because they are expected to cascade to even smaller scales anyway, it is desirable to remove these waves." In yet another recent paper one

reads that "Unwanted noise is generated in numerical weather prediction models, by the orography, by the boundaries, by the "physics," or even sometimes by the dynamics. The spectral approach provides two useful filters for attacking this problem *at no computational cost*. ... It was now necessary to write and test new filters for the gridpoint model if it was to continue to compete with the spectral model."

I will return to some of these issues in more detail in the continuation of this lecture. For examples of physical properties that have been and can be considered in the Arakawa style I will start with a retrospective of the horizontal grid topic. This will permit me to review and also present some recent developments in this area. I will proceed with an exposition on the experience from the operational running of the Eta Model at the U.S. National Centers for Environmental Prediction (NCEP), to the extent that it can be viewed as a contribution to the issues raised. I will proceed to a number of other global and limited area modeling topics, having to do with the pole problem, the viability of the limited area modeling approach, and the resolution vs domain size trade-off. Use will again be made of the Eta Model results when appropriate. I will conclude by illustrating the remarkable progress in the atmospheric numerical modeling field that has been accomplished; and by commenting on thrusts taking place or expected.

2. The horizontal grid: Retrospective

Choice of the horizontal grid could well be considered the central point of the Arakawa-style considerations as numerous issues and trade-offs are involved related to one choice or another. It is also the first problem that received attention at the beginning of the "primitive equation age" of atmospheric modeling in the late sixties.

In a primitive equations framework, AL have argued that there are two main computational problems in the simulation of atmospheric motions: simulation of the geostrophic adjustment, and simulation of the slowly changing quasi-geostrophic motion after it has been established by the geostrophic adjustment. As to the former, Winninghoff (1968) and AL have analyzed the dispersion properties of the simplest centered approximations to the shallow-water equations on square horizontal grids. Their results have subsequently been summarized and/or discussed at a number of places (e.g., Janjic and Mesinger, 1984), most recently probably by Randall (1994); and will only briefly be stated here. The desirable property of the relative frequency monotonically

increasing with wavenumber is achieved only for some of the grids and for some values of λ/d, λ being the radius of deformation, $(gH)^{1/2}/f$, with symbols here having their usual meaning; and d the grid distance. The results for the nonstaggered grid, A, and the fully-staggered grid D, having u and v located so that they represent velocity components tangential to h-point grid boxes, turn out to be rather unfavorable. The fully-staggered grid C, having u and v located to represent components normal to h-point boxes, and the semi-staggered grid, B and/or E, having the two velocity components at the same points, look much better. To quote Randall (1994), "the C grid does well with deep, external modes but has serious problems with high internal modes, whereas the B grid has moderate problems with all modes."

Irrespective of how much one or the other type of modes are present in the real atmosphere, the problem of deep external modes seems quite important in primitive equation models. With "physics" performed in individual grid boxes of the model, note that 29 % of the heat resulting from a physics call will instantaneously be converted into the gravitational potential energy of the column. If, in a thought experiment, we consider a single column having received heat in this way, it will as a result have an excess of potential energy relative to surrounding columns. This will generate outward-directed pressure gradient forces which will initiate a geostrophic adjustment process. How satisfactorily a process is handled which is initiated by this fraction of heat supplied by a physics call should certainly be a subject of concern.

With the B grid, as pointed out by Arakawa (1972), it is the averaging of the pressure gradient force which is the cause of the trouble. With the E grid representing the B grid rotated by 45 degrees, the problem is the same except that the averaging is not explicitly performed; shallow-water pure gravity-inertia wave solutions on the two grids are in fact identical (Mesinger and Arakawa, 1976). The two grids will therefore be referred to as the B/E grid hereafter when statements made are applicable to both of them.

The propagation of the pure shallow-water gravity-wave is the source of the geostrophic adjustment difficulties of grids other than C. Consider the B/E grid: it can be considered as consisting of two C subgrids, shifted by the B/E-grid grid distance relative to each other. If now a single h point is perturbed, a pure gravity wave that is excited will propagate only along points of a single C subgrid to which the perturbed point belongs. Points of the other C subgrid, which include the four h points nearest to the perturbed point, will not be affected. This is the lattice-separation problem of the B/E grid. In a more complete system the four h points nearest to the

perturbed point will be affected, but only through much slower Coriolis and advection terms (Mesinger, 1973). The situation with the A and the D grid, in this sense, is still worse, and will not be further considered here.

Lattice separation is a problem of space differencing. This can also in a formal way be demonstrated by considering the phase speed of a pure gravity wave, with the time derivative left in the differential form and space derivatives replaced by simplest centered analogs. For the E grid, one obtains (e.g., Mesinger and Arakawa, 1976),

$$\frac{c_*}{\sqrt{gH}} = \sqrt{\frac{\sin^2 X + \sin^2 Y}{X^2 + Y^2}} \quad . \tag{2.1}$$

Here c_* is the finite-difference phase speed, $X \equiv kd/\sqrt{2}$, $Y \equiv ld/\sqrt{2}$, with k, d, and the remaining symbols having their usual meaning. The contour plot of (2.1) is shown in Fig. 1; because of symmetry only one half of the admissible wavenumber domain is displayed. The relative phase speed is seen to reduce to zero for the highest admissible wavenumber of the domain displayed, $X = \pi$. Constant values of h on one and on the other of the C subgrids, different from each other, represent a stationary solution, no matter how different the two values might be.

To address this B/E grid lattice separation problem, Arakawa (1972) designed a time-alternating-space-uncentered scheme, which he had used in combination with the Matsuno time differencing. A method of arriving at space-time centered, second-order accurate schemes was subsequently proposed by Mesinger (1973; see also Mesinger and Arakawa, 1976). The method results in modifications of the divergence term of the continuity equation. Specifics of the modification will depend on the choice of the time-differencing scheme; but will entail interaction between neighboring height points via the pure gravity wave terms, thus significantly improving on the lattice-separation problem. If, for example, the forward-backward time scheme is used, with the momentum equation integrated forward,

$$u^{n+1} = u^n - g\Delta t\,\delta_x h^n, \qquad v^{n+1} = v^n - g\Delta t\,\delta_y h^n \,, \tag{2.2}$$

instead of

$$h^{n+1} = h^n - H\Delta t\left[\left(\delta_x u + \delta_y v\right) - g\Delta t\,\nabla_*^2 h\right]^n, \tag{2.3}$$

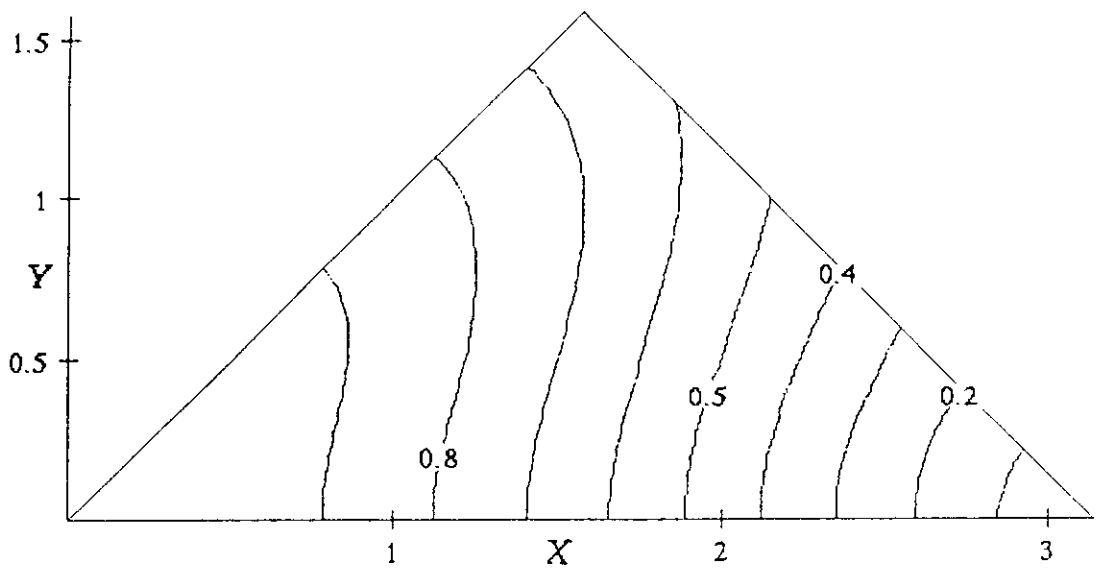

Fig. 1. Relative phase speed of gravity wave with simplest centered space differencing, (2.1), on the Arakawa E grid. For reasons of symmetry, only a half of the admissible wavenumber domain is shown.

the method results in the continuity equation (Mesinger, 1974)

$$h^{n+1} = h^n - H\Delta t\left[\left(\delta_x u + \delta_y v\right) - g\Delta t\left(\frac{3}{4}\nabla_+^2 h + \frac{1}{4}\nabla_\times^2 h\right)\right]^n . \qquad (2.4)$$

Here again the E grid is used, n is the time index, and substitutions have been made from (2.2) into (2.3) and (2.4) so as to have on their right sides values at the time level n only; the "plus" and the "cross" subscripts depict the geometry of the h values used in five-point analogs to the Laplacian; and other symbols have their standard meaning. The original system (2.2) and (2.3) involves no communication between the two C subgrids of the E grid. In contrast, in the system (2.2) and (2.4), this communication is achieved via the cross Laplacian term of (2.4).

For visualization of the impact of this difference, consider what happens following an increase in height at a single height point, within one forward-backward time step. With the system (2.2) and (2.3), height values at second nearest neighbors increase, as depicted by the plus Laplacian of (2.3); while the four nearest h-point neighbors undergo no change. When (2.3) is replaced by (2.4), height values at all eight neighbors will increase, a much more satisfactory situation. Still, the h values at the four nearest neighbors, belonging to the C subgrid which is not the one of the perturbed point, will undergo an increase which is only two-thirds of that which occurs at the second nearest neighbors. Thus, while the improvement due to the modification is considerable, it is not one which has completely removed the problem. Besides, the modification also results in some damping of the shortest gravity waves (e.g., Mesinger, 1974). Returning to the positive side, one can take additional comfort in the facts that the scheme remains neutral for waves for which the wavenumbers in the x- and in the y-direction are the same, that the modification has no impact when the plus and the cross Laplacians are equal, and that there is no penalty in terms of the CFL stability condition of the scheme.

There are understandably numerous other considerations to be made in assessing the attractiveness of the C vs the B/E grid. Regarding the "slowly changing quasi-geostrophic motion" the highest priority of course has been accorded to the horizontal advection scheme resulting in the Arakawa-Lamb (1981) scheme for the C grid, and in the Janjic (1984) scheme for the B/E grid. Both schemes reduce to the Arakawa (1966) scheme in the case of horizontal nondivergent flow, and accordingly have their analogs of the famous Fjørtoft-Charney energy scale (e.g., Mesinger and Arakawa, 1976, Fig. 7.1). Energy scale analogs are different however,

with the Janjic scheme analog having the two-grid-interval wave extend to infinity so that the cascade into the shortest wave is not possible (Janjic and Mesinger, 1984, Fig. 3.12). This results in an enhanced constraint on the energy cascade into the smallest scales. Still other differences between the two schemes are their conservation properties that are additional to the three classical ones of the Arakawa (1966) scheme with the Arakawa-Lamb scheme conserving potential enstrophy, and the Janjic scheme conserving momentum. Thus, with the Janjic scheme, the Hollingsworth-Källberg noncancellation instability (Hollingsworth et al., 1983) is not a matter of concern.

Time differencing is yet another consideration. The leapfrog or the semi-implicit scheme are the choices typical of the C grid models, and the split-explicit, forward-backward scheme of the B/E grid ones. Attractiveness of the simple two-time level split-explicit scheme, if one were to be a believer in it, is with the C grid reduced due to a problem with the Coriolis terms.

My choice of the E grid when writing the code which could be considered the ancestor of the today's Eta Model (e.g., Mesinger and Janjic, 1974) was based on two additional points. One is the simple appeal of carrying the two velocity components at the same grid points, given that it is the velocity vector which is the basic dynamical variable to be forecast, and not its individual components.

The second is the possibility of having all variables defined along a single outer boundary of an E-grid limited-area domain. This feature has enabled the design of an apparently very successful lateral boundary conditions scheme (Mesinger, 1977) along the lines of Oliger and Sundström (1978); this point will be returned to later in the lecture.

3. Hexagonal grids

With each of the square grids and centered second-order schemes experiencing a set of problems, examination of other options is obviously justified. An option considered early in the development of the primitive equation techniques has been that of the hexagonal grids. One might argue that the hexagonal grid is an attractive choice given that each grid point has a set of six nearest neighbors, with all six at the same distance from the considered point, being isotropic in that sense.

All four of the Arakawa grids have their hexagonal analogs. They are displayed in Fig. 2,

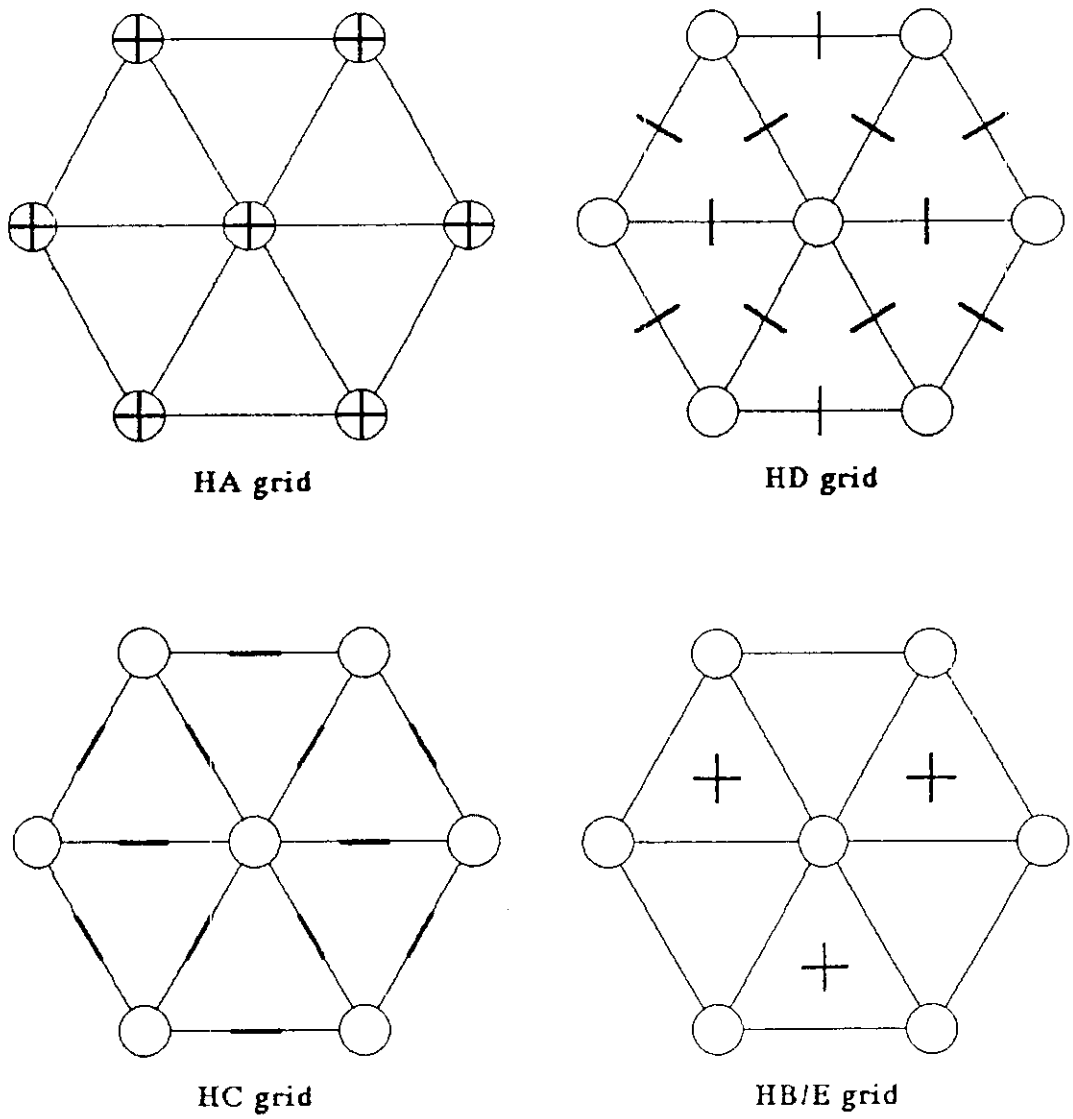

Fig. 2. Hexagonal analogs of the Arakawa square horizontal grids A, D, C and B/E. Circles denote the h points, and bars denote the location as well as orientation of the velocity components.

using circles to denote the height points, and bars to depict the location as well as orientation of the velocity points (in the manner of Song and Tang, 1991, personal communication). In the order as displayed, they will be referred to as the HA, HD, HC, and the HB/E grid. In their very early work Sadourny and Williamson used the first three of the "H" grids, as shown here; Sadourny the D and then the C grid, and Williamson the A grid (e.g., Sadourny and Morel, 1969, Williamson, 1969, and references therein). The somewhat counter-intuitive HB/E grid has been used by Thacker (e.g., 1978).

A disadvantage of the fully-staggered grids D and C specific to their hexagonal versions is their having an excess of velocity components, three components per each height point rather than two (Sadourny, personal communication). To circumvent this disadvantage still another possibility has been pointed out by Popovic et al. (1996), to skip every third velocity component of the HC grid. One ends up with a grid which can be obtained by deforming a square C grid into a hexagonal shape.

At the time of the early work of Sadourny and Williamson little was known about the properties of the finite-difference analogs of primitive equations on various grids as summarized here and the question arises what is the situation with the hexagonal grids regarding the issues raised. This was precisely the idea of Nickovic (1994) when he recently analyzed the stability of the forward-backward scheme used on the HC grid. He has found that the scheme is neutral provided

$$\Delta t \leq \sqrt{\frac{2}{3}}\,\frac{d_h}{\sqrt{gH}}\,, \tag{3.1}$$

where d_h is the hexagonal grid distance. For a possible comparison with the stability ranges of the square grids, one should note that

$$d_h = \sqrt{\frac{2}{\sqrt{3}}}\,d\,, \tag{3.2}$$

where d is the grid distance of an equivalent square-grid having the same number of grid points per unit area. The numerical factor on the right side of (3.2) is equal to about 1.075. A point emphasized by Nickovic is that the hexagonal grid used on an icosahedron to construct grids for the sphere may have caused concern due to its singular points and lines, but that this would not stand in the way of using a hexagonal grid for a limited area model.

In view of the HC grid problem of the extra velocity components that is additional to the standard C grid problem of the need for averaging of the Coriolis terms, properties of the HB/E grid appear particularly intriguing. As to the forward-backward scheme, using the simplest three-point differencing for the gravity wave terms one can demonstrate that the scheme corresponds to the centered second-order wave equation. The scheme is neutral within the same stability range as that of the HC grid scheme, (3.1). With the time derivative kept in the differential form, the relative gravity-wave speed is

$$\frac{c_*}{\sqrt{gH}} = 2\sqrt{\frac{3-\cos X-2\cos(X/2)\cos(\sqrt{3}Y/2)}{3\,(X^2+Y^2)}}\ . \qquad (3.3)$$

Here $X = kd_h$, $Y = ld_h$, with k and l as before being the wavenumbers along the x- and the y-axes. The admissible wavenumber domain of the hexagonal grid is shown in the upper panel of Fig. 3, and the relative phase speed (3.3) in its lower panel. Because of the three-fold symmetry within the positive wavenumber quadrant, only one-third of the admissible domain is shown. In contrast to Fig. 1, the relative phase speed is seen never to reduce to zero; its minimum value is $(3/2)^{3/2}/\pi$, about 0.585. There is no lattice separation problem.

These attractive features of the HB/E grid, perhaps also of the HC grid, call for additional attention. The geostrophic adjustment situation in the Arakawa-Winninghoff sense has been analyzed by Nickovic (1998, personal communication). The relative frequency, $|\nu|/f$, of the gravity-inertia wave Nickovic obtains for the HC grid, for the case $\lambda/d = 2$, is shown in the upper panel of Fig. 4. The values seen are similar to those of the square C grid (e.g., Arakawa and Lamb, 1977); the relative frequencies increase inside all of the admissible wavenumber domain, attaining maximum values at its corners. In the lower panel of the figure, relative frequencies of the geostrophic mode are shown. They are different from zero, in striking contrast to the situation with any of the square grids.

The situation is similar with the HB/E grid (not shown), with an additional feature that the relative frequencies of the two gravity-inertia waves are somewhat different. Once again an error in the frequency of the geostrophic mode is found.

How damaging the error in the frequency of the geostrophic mode discovered by Nickovic might be is obviously an important issue. To my knowledge there are no comprehensive model integrations, in a hexagonal u,v formulation, which could be used for an attempt to answer this

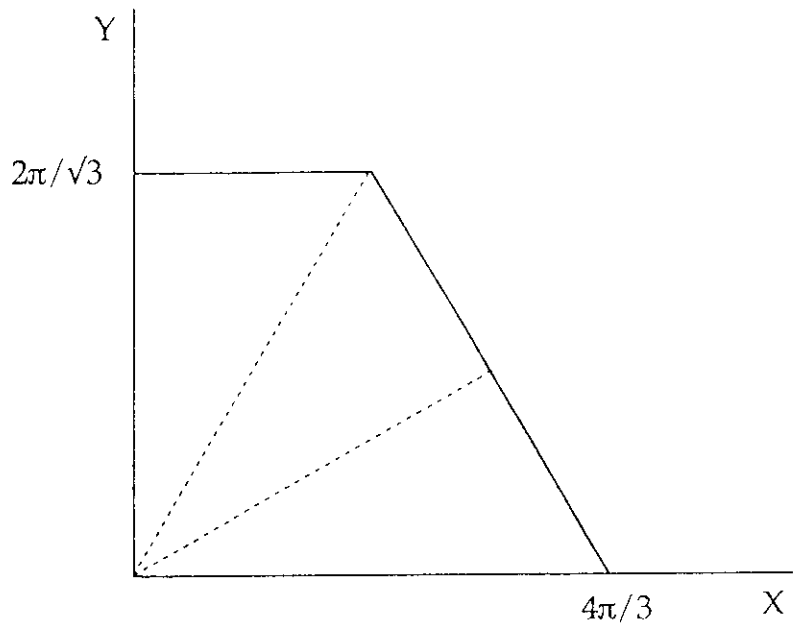

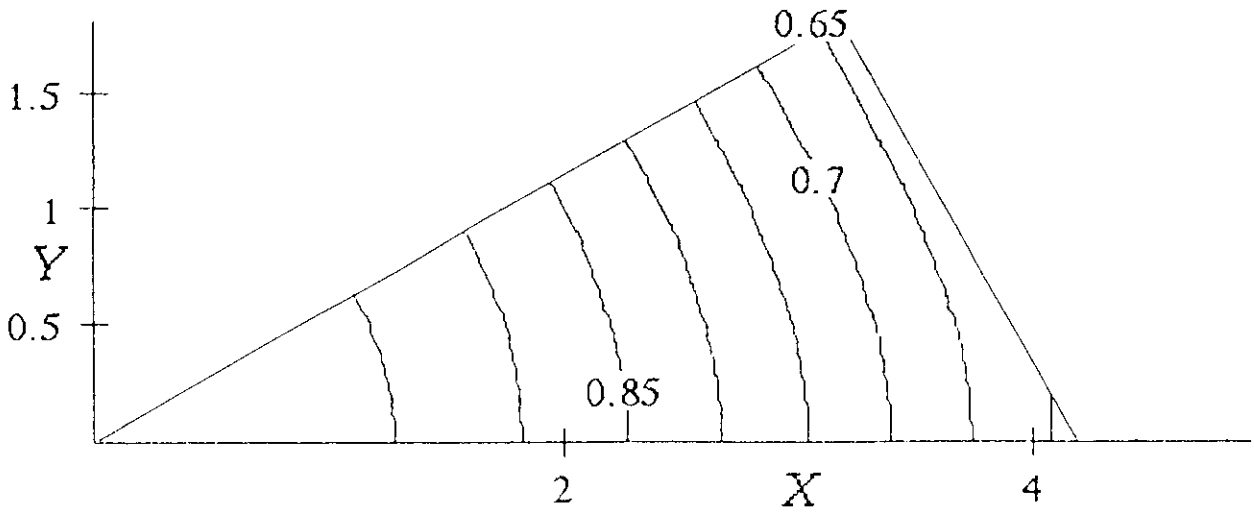

Fig. 3. The admissible wavenumber domain of the hexagonal grid, upper panel, with $X \equiv kd_h$, $Y \equiv ld_h$. Here d_h is the grid distance of the hexagonal grid. Relative phase speed of gravity wave with simplest centered space differencing, (3.3), on the hexagonal B/E grid, lower panel. For reasons of symmetry, only a third of the admissible wavenumber domain is shown.

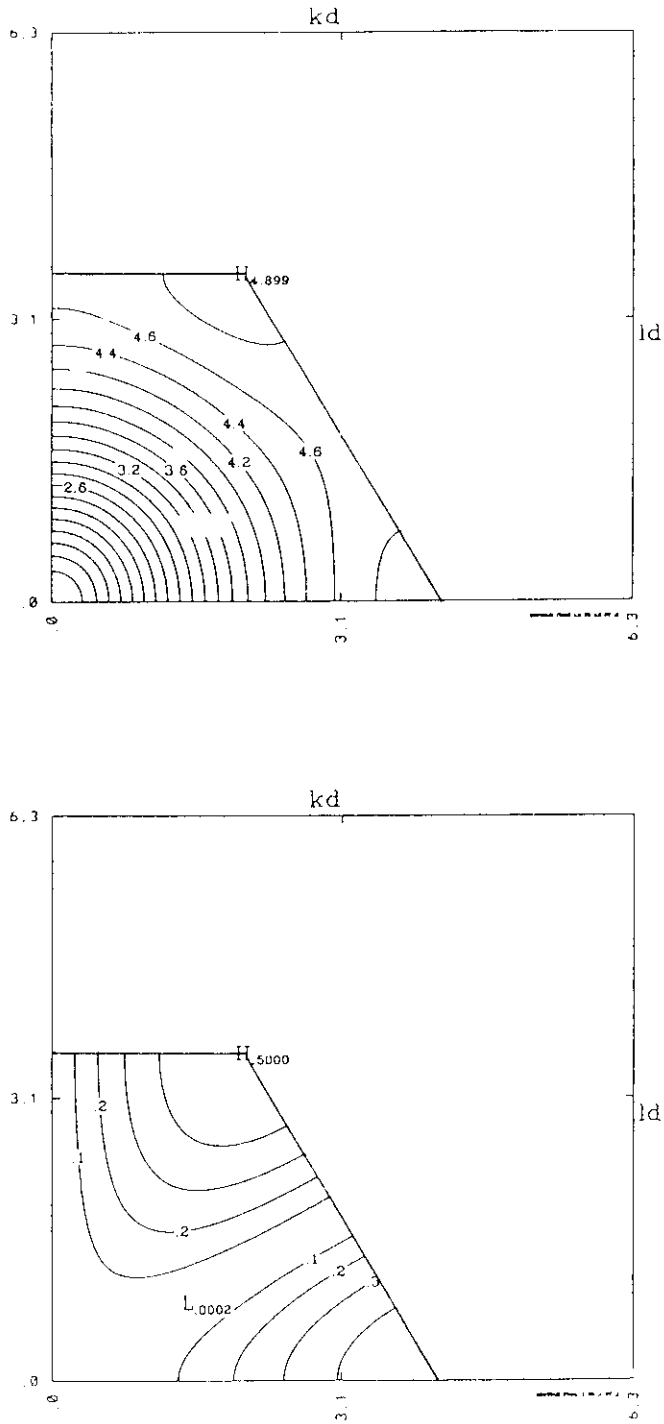

Fig. 4. The relative frequency, $|\nu|/f$, on the HC grid with simplest centered space differencing, for the case $\lambda/d = 2$. The gravity-inertia wave relative frequency is shown in the upper panel, and that of the geostrophic mode in the lower panel (Ničković 1998, personal communication).

question. In the source-sink experiment of Nickovic (1994) no detrimental effects were obvious; the result looked encouraging.

4. Randall Z grid, and C-grid-like B/E grid gravity wave schemes

Excellent geostrophic adjustment properties of the unstaggered grid for the vorticity and divergence as prognostic variables ("Z" grid) were pointed out by Randall (1994). Progress in using the vorticity/divergence formulation on a hexagonal grid, subsequent to Heikes and Randall (1995a, 1995b) are reported elsewhere in this volume.

Still another option is to try to benefit from both the simplicity and straightforwardness of the u,v formulation and from the excellent properties of the streamfunction/velocity potential formulation for gravity-inertia waves, by switching between the two as the integration proceeds. The cost of this option in view of the need to solve for the streamfunction and for the velocity potential at each time step may appear discouraging at this time.

A radically new approach to address the lattice-separation problem has however been advanced by Janjic (1992, personal communication; also Janjic et al., 1998). It consists of averaging the time difference in the continuity equation. If, for example, the forward-backward scheme is used with the continuity equation integrated forward, on the B grid, and the averaging is performed over five points, we have

$$u^{n+1} = u^n - g\,\Delta t\,\delta_x(\bar{h}^y)^{n+1}\,,$$
$$v^{n+1} = v^n - g\,\Delta t\,\delta_y(\bar{h}^x)^{n+1}\,, \tag{4.1}$$

$$\tfrac{1}{2}(\bar{h}^{xx}+\bar{h}^{yy})^{n+1} = \tfrac{1}{2}(\bar{h}^{xx}+\bar{h}^{yy})^{n} - H\,\Delta t\,(\delta_x\bar{u}^y + \delta_y\bar{v}^x)^n\,. \tag{4.2}$$

I shall refer to the scheme as the "five h-point", or FHP scheme. As shown by Janjic, the scheme is neutral for

$$\Delta t \le \frac{d}{\sqrt{2gH}}\,, \tag{4.3}$$

which is the same as the C-grid stability condition. With the time derivative in the differential form, the relative gravity wave speed is

$$\frac{c_*}{\sqrt{gH}} = \sqrt{2\,\frac{\sin^2 X \cos^2 Y + \cos^2 X \sin^2 Y}{(X^2+Y^2)(\cos^2 X + \cos^2 Y)}}\,. \tag{4.4}$$

Here $X = kd/2$, $Y = ld/2$. Within the admissible wavenumber domain, (4.4) achieves its minimum value for $X = \pi/2$, $Y = \pi/2$, of about 0.65. Thus, there is no lattice separation problem.

On the downside, "deaveraging" (Janjic et al., 1998) of (4.2) needs to be performed; this can be done by relaxation which according to Janjic et al. (1998) converges "surprisingly quickly". A single-point height perturbation affects in a single time step the four nearest height points the most (a "C-grid-like" scheme), but propagates in one time step throughout the domain. This is reminiscent of the situation with the so-called compact schemes (e.g., Leslie and Purser, 1991).

Yet another scheme can be easily designed which will also employ tendency averaging to remove the B/E grid lattice separation problem. This can be done by essentially following the idea of Janjic (1984) for his construction of the B/E grid horizontal advection scheme. First, auxiliary C-grid velocity components are introduced in an appropriate way. For the gravity wave terms they are needed midway between the nearest height points on the B grid so as to be defined by

$$u_C = \bar{u}^y, \qquad v_C = \bar{v}^x\,. \tag{4.5}$$

If now the forward-backward scheme is desired, one can write the scheme in terms of the C-grid velocities, and then substitute (4.5) to obtain a B-grid scheme. If the continuity equation is integrated forward, one obtains

$$\begin{aligned} (\bar{u}^y)^{n+1} &= (\bar{u}^y)^n - g\,\Delta t\,\delta_x h^{n+1}\,, \\ (\bar{v}^x)^{n+1} &= (\bar{v}^x)^n - g\,\Delta t\,\delta_y h^{n+1}\,, \end{aligned} \tag{4.6}$$

$$h^{n+1} = h^n - H\,\Delta t\,(\delta_x \bar{u}^y + \delta_y \bar{v}^x)^n\,. \tag{4.7}$$

The scheme is neutral for

$$\Delta t \le \frac{d}{\sqrt{2gH}}\,, \tag{4.8}$$

which is once again the C-grid stability condition. The relative gravity wave speed, with the time derivative in the differential form, is

$$\frac{c_*}{\sqrt{gH}} = \sqrt{\frac{\sin^2 X + \sin^2 Y}{X^2 + Y^2}}\ , \tag{4.9}$$

with X and Y having their B-grid definitions, as in (4.4). Contour plots of the relative gravity wave speeds of the two schemes, (4.4) and (4.9), are shown in Fig. 5. With the admissible domains of both X and Y being $\leq \pi/2$, the minimum value of (4.9) is once more seen to be about 0.65. There is no lattice separation problem. In fact, (4.9) can be recognized as identical to the gravity wave speed on the C grid (e.g., Mesinger and Arakawa, 1976) which may come as no surprise given the way the scheme has been designed. Inspection of the C-grid system used to arrive at (4.6)-(4.7) shows that a height change at a single point will in one time step propagate to the four nearest neighbors and to no other height points, as on the C grid. A "simulated C-grid" scheme, SCG, seems thus appropriate for (4.6)-(4.7).

How can this happen that on the B grid propagation of a single-point height perturbation takes place the same as on the C grid? With velocities at time step n zero, and heights constant except for a single grid-point value -- for example higher than the others -- solution of (4.6) results in a wind field at the level n+1 as depicted in Fig. 6. Additional to the velocities directed radially away from the perturbed point, two strips of velocity components are created as needed to have the resulting velocity divergence different from zero at all h-points except at the perturbed point and its four nearest neighbors.

Additional to the need for deaveraging, the cost for achieving a C-grid-like propagation of single-point height perturbations is thus for both schemes a spurious wave created throughout the domain; for the FHP scheme in the height field, and for the SCG scheme in the velocity field. The constant amplitude of the spurious velocities shown in Fig. 5 may look worrisome; one could take some comfort in the idea that these velocities would be invisible to the Coriolis terms if the Coriolis terms were also to be included via the two point averaging in (4.6).

Source-sink experiments à la Arakawa (1972) were performed for both schemes (Gavrilov, 1998, personal communication). Both schemes gave expected results (e.g., Janjic and Mesinger, 1989) and were efficient in the sense that relaxation to solve for the h or the u,v tendencies was converging quickly. Thus, no preference for one or the other of the two schemes was obvious. It was recently noted by Nickovic (1997, personal communication) that five-point-averaging of the velocity-component tendencies also results in a scheme with gravity-wave properties the same as those of the FHP scheme.

A favorable feature of this class of "tendency averaged schemes" is that they can be tested in a comprehensive split model by simply replacing its adjustment stage by a stage based on one or the other of the schemes summarized. One effort of this kind, by Janjic et al (1998), was already referred to. But apart from prospects offered by specific schemes or approaches reviewed in this and in the preceding section, one purpose of the material presented was to illustrate the variety of possibilities one can explore in trying to achieve the behavior of the difference scheme which is appealing from the physical point of view. Only issues related to the choice of the horizontal grid were considered; there are of course many others. Some will be touched upon in the following sections, but from a different perspective, namely that of the design and performance of a specific model.

5. The Eta Model: an Arakawa approach story

The so-called Eta Model is a limited-area model with the numerical formulation designed following the Arakawa principles. It has been used so far primarily for weather forecasting, so one could question the appropriateness of covering it within the symposium carrying the general circulation model (GCM) development title.

My reasons for finding this appropriate are twofold. The first is that nowadays limited-area models are increasingly used as integral parts of general circulation models, for simulation of regional climate. A very successful recent Eta Model example of such a use is that of Ji and Vernekar (1997). Use of the Eta nested within a GCM led to dramatic improvements in their simulation of a number of observed features of Asian monsoons, compared to results of the GCM with no Eta nest.

The second is that a forecasting model is an excellent vehicle for testing the performance of a scheme or a set of schemes. In a typical operational setting, forecasts are initialized twice daily and verified against analyses. A large body of verification statistics tends to be automatically accumulated. "Clean" experiments can be and are set up in which a model with a single change is compared against the control (e.g., Rogers et al., 1996, Mesinger et al., 1997, and references therein). Also, performance of forecasting models with different properties are regularly compared and inferences made.

I expect to be able to contribute to this class of assessments, and specifically to that of the

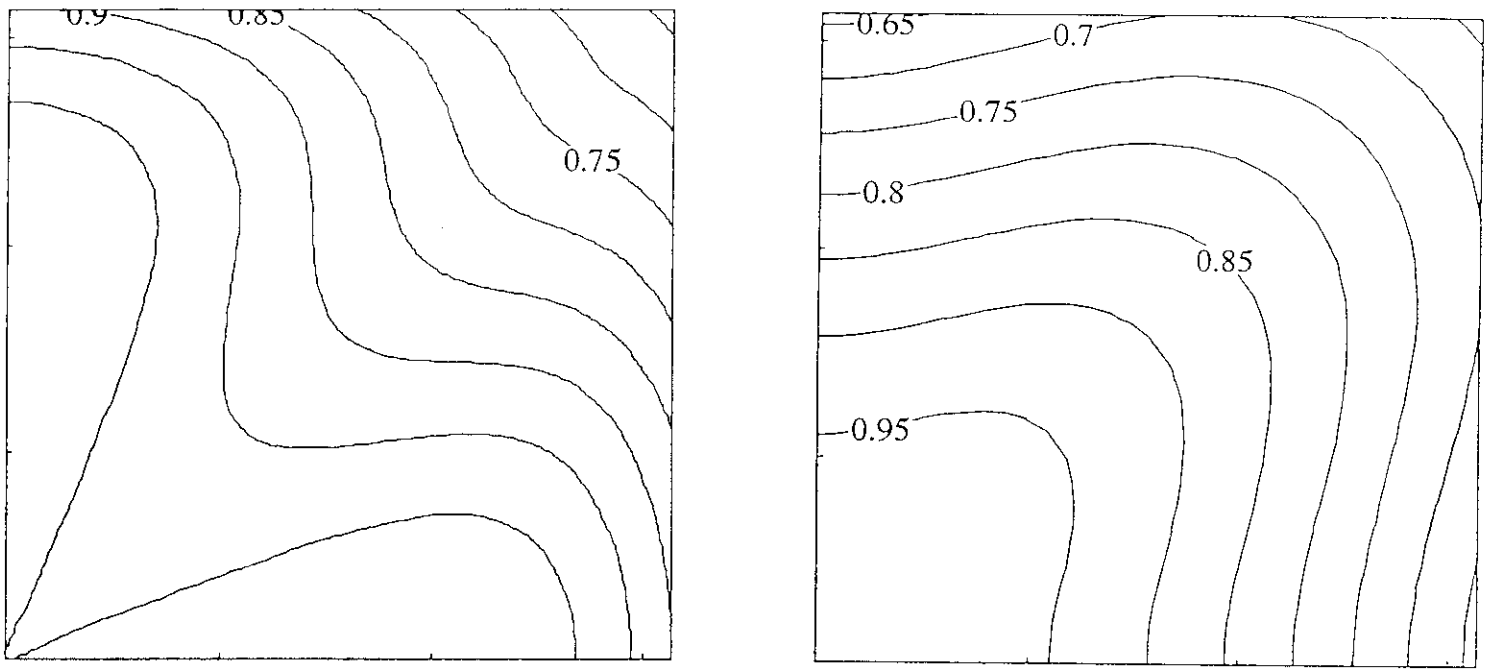

Fig. 5. Relative gravity wave speed of the Janjic "five h-point" scheme, (4.1)-(4.2), left panel; and of the "simulated C-grid" scheme, right panel; on the B grid, and with time derivatives in the differential form. The coordinate axes are $X \equiv kd/2$, $Y \equiv ld/2$.

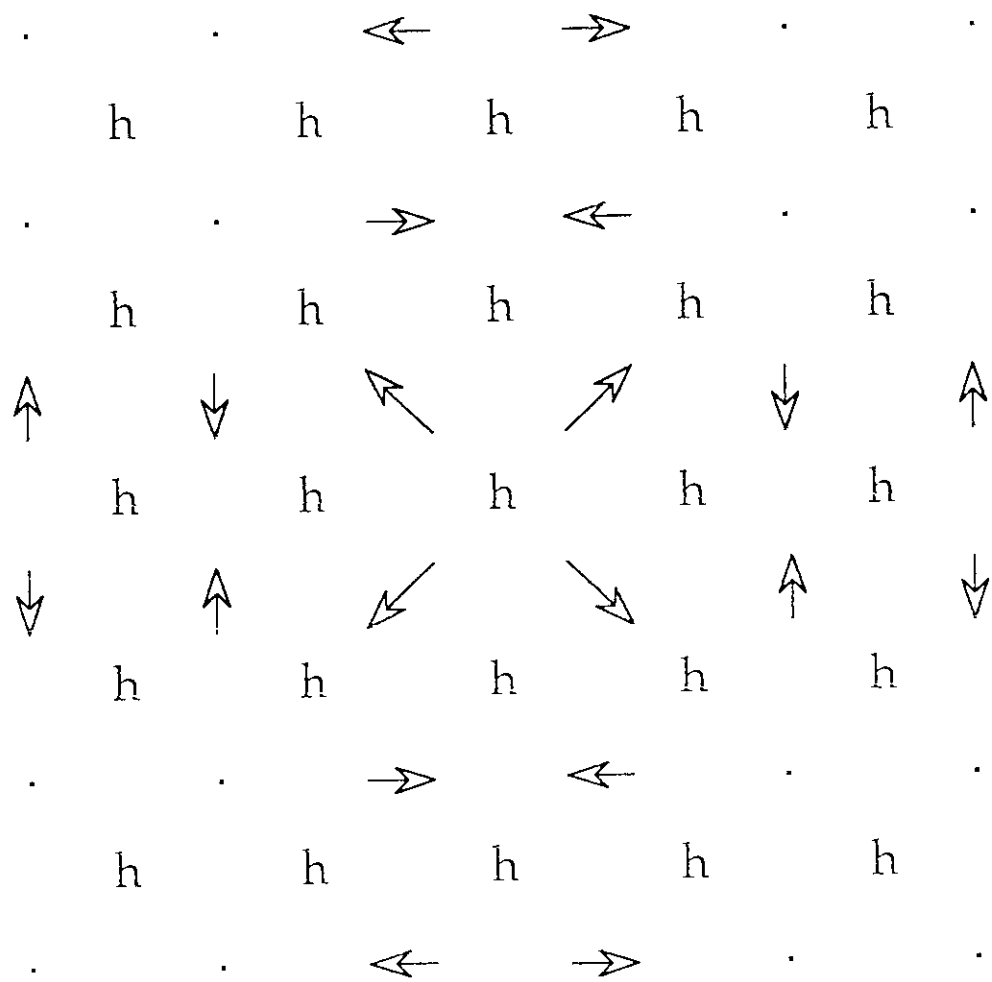

Fig. 6. Solution of the B-grid "simulated C-grid" scheme, (4.6)-(4.7), for the wind field at time level n+1, following an initial condition of the velocities at time step n equal to zero, and heights constant except for a single grid-point value, that at the center of the plot, higher than the others.

impact of the Arakawa vs what might perhaps be called a traditional approach, by reviewing some of the results of the Eta Model in the remainder of this lecture. Expectation may have been widespread that the maintenance of the integral constraints and other Arakawa-type properties of the difference system while very important in climate integrations may not be a critical requirement for short-range forecasting, and that the local accuracy in short-range predictions is therefore more or less determined by the grid size and the order of accuracy of the scheme. I find that evidence accumulated during the past decade or two shows that this expectation was not justified; in fact, short-range forecasting as I hope to demonstrate may well have resulted in the most convincing indication of the potential of the approach.

There is, of course, no unique way to design the dynamics of a model following the Arakawa principles, and some of the principles may be more rewarding than others. Moreover, as the review of the horizontal grid issues shows, trade-offs are typically encountered and the best choice is frequently not obvious. A summary of the Eta Model features is thus necessary. Of the various unique features of its numerical formulation, most deserving of being noted in my opinion are the following.

- The step-mountain ("eta") vertical coordinate (Mesinger, 1984; see also Mesinger et al., 1988). The surfaces of constant eta are approximately horizontal, thereby avoiding the cause of the notorious sigma system pressure-gradient force problem (e.g., Mesinger and Janjic, 1985). Perhaps just as importantly, to simulate horizontal motion over large-scale mountain ranges, there is no need for the model to generate vertical velocities through coordinate surfaces on one and on the other side of the mountain range;

- The Janjic (1984) Arakawa horizontal momentum advection scheme. On the model's E-grid, the scheme conserves C-grid defined enstrophy for horizontal nondivergent flow. As summarized in Section 2, this results in an enhanced constraint on the energy cascade toward smaller scales. Numerous other quantities are conserved, including momentum apart from the effect of mountains;

- Gravity-wave coupling scheme of Mesinger (1973, 1974) and Janjic (1979). Rather than the scheme (2.2) and (2.4), the version of the modified forward-backward scheme with the continuity equation integrated forward is used (Janjic, 1979). Integration of the continuity equation forward requires less storage than the integration of the momentum equation forward, and for pure gravity-wave terms results in the same difference analog of the wave equation;

• Energy conservation in transformations between the kinetic and the potential energy in both space and time differencing (Mesinger, 1984, Mesinger et al., 1988, Janjic et al., 1995);

• Lateral boundary conditions prescribed/extrapolated along a single outer boundary line, followed by a "buffer" row of points of four-point averaging (Mesinger, 1977). The four-point averaging achieves coupling of the boundary conditions of the two C-subgrids. Model integration from the third row of points inwards is done with no "boundary relaxation" or enhanced diffusion zone ("fairly well-posed" lateral boundary conditions according to McDonald, 1997).

Within the model's physics package some of the special features are its modified Betts-Miller convection scheme (Janjic, 1994), its Mellor-Yamada level 2.5 turbulence closure with improved treatment of the realizability problem (Mesinger, 1993, Janjic, 1996a), its viscous sublayer scheme over both water and land surfaces (Janjic, 1996b), and its prognostic cloud water/ice scheme (Zhao and Carr, 1997).

Until October 1995, the model was initialized with a static "regional" optimum interpolation (ROI) analysis using the Global Data Analysis System (GDAS) first guess (Rogers et al., 1995). As of 12 October 1995 until February 1998, this was replaced by a 12-h Eta-based intermittent asimilation (EDAS; Rogers et al., 1996). More information on model's physics package and its initialization/assimilation, and verification system can be found, e.g., in Janjic (1994), Black et al. (1993) and Rogers et al. (1996).

Models change. It should be stressed however that what I believe would generally be considered major features of a model's numerical design, have not changed in the Eta's case since the mid-eighties when the minimum physics version of the eta coordinate code was put together. This includes the five features described in the summary above.

The Eta Model was operationally implemented at the then National Meteorological Center (NMC) on 9 June 1993, as the so called NMC early run. The term "early" refers to an early data cutoff, of 1:15 h, aimed at providing guidance as quickly as possible. The name "Early Eta" came into widespread use after the implementation of a later run of the Eta, at higher resolution, the so-called "Meso Eta", in 1995.

For a regional model to be implemented at an operational center already running an operational regional model, as the NMC was at the time, the new model clearly needs to demonstrate a superior performance; or at least an obvious potential of one. Given the existence

at NMC then as now also of an operational global model, this automatically implies an advantage of some kind as well over the NMC's global model product as available at the forecast time of the regional model. Namely, without such an advantage of the regional over the global model, running a separate regional model would be hard to justify.

The two models against which the Eta is thus naturally compared are the so-called Nested Grid Model (NGM), and the Medium Range Forecasting (MRF) or Aviation (Avn) model. The NGM, or Regional Analysis and Forecasting System (RAFS) when referring to the entire forecast system containing the model, is a sigma coordinate gridpoint model, with an approximately 80-km inner grid nested inside its own coarser outer grid. Both grids have 16 layers in the vertical. It is initialized with a 12-h NGM-based intermittent assimilation using ROI analysis, with a 2:00 h data cutoff (DiMego, 1988). No change in the model nor in its analysis system have been made since August 1991 (DiMego et al., 1992). The model however continues to be run twice daily, off 0000 and 1200 UTC data, 48 h ahead.

The Avn/MRF model is a global spectral sigma system model. Since August 1993 it is run with the triangular 126 truncation (T126), and 28 layers (e.g., Kanamitsu et al., 1991; Pan and Wu, 1994; Hong and Pan, 1996). The two names, Avn and MRF, refer to the same model but to different data cutoff times: until very recently, twice daily, at 0000 and 1200 UTC, the model was run 72 h ahead with an early data cutoff, of 2:45 h, under the name Aviation model; at 0000 UTC the Avn run is followed by the MRF Model run with a later data cutoff, of 6:00 h. The Avn model forecasts are used for the Eta boundary conditions; however, since the Eta runs first, the 12-h old Avn run has been used. This has changed in February 1998 as a result of the implementation of four runs per day of ther Avn model.

Ever since the early development stage and through its now more than four and a half years of operational running, precipitation scores were perhaps the main guidance in assessing the overall Eta performance and in deciding on model changes. The precipitation analysis system of the NCEP's Environmental Modeling Center (EMC) used for that purpose is based on data provided by the National Weather Services's River Forecast Centers (RFCs); these consist of reports of accumulated precipitation for each 24-h period ending at 1200 UTC. The analysis covers the area of the contiguous United States with reports from about ten thousand RFC rain gauge stations. In areas of poor coverage, RFCs data are augmented by radar precipitation estimates if rain gauge data are available to calibrate the radar data. Data are analyzed to the

grid-boxes of the verification grid by simple grid-box averaging. With verification grid size on the order of 80 km, about ten reports are available per verification box.

Three-model scores, of the Eta, the Avn/MRF model, and the NGM, and for three verification periods, 00-24, 12-36 and 24-48 h, are available and archived beginning with September 1993. Since the relative model performance is to some extent season-dependent, it is necessary to look at full 12-month samples, or multiples of 12 months, if the seasonal model performance is not to have an impact on the result. Accordingly, in Fig. 7, equitable threat and bias scores for the three models and for the first 24-months of the available scores, September 1993-August 1995, are shown. Recall that equitable threat score is the standard threat score corrected for skill of a random forecast, e.g., Mesinger (1996b). The motivation for displaying the result for a 24-month sample is that during that time the resolution of the Eta Model remained unchanged, at approximately 80 km in the horizontal and 38 layers in the vertical.

There are two points I wish to make based on the results shown in the figure. For the first, note that for all the precipitation categories monitored the Eta threat scores are higher than those of its "driver" Avn/MRF model. This happens in spite of the Eta handicaps of using 12-h "old" Avn boundary conditions, and having a shorter data cutoff, so that the Eta forecasts initialized at a given time are available before those of the global model. The Eta results thus confirm the validity of the regional limited-area modeling approach, showing that increased forecast accuracy is achieved using a limited area model.

For the second point, I wish to emphasize that the NGM employs fourth-order accuracy schemes, along with a periodic application of a fourth-order Shapiro filter (Juang and Hoke, 1992). Its resolution and its overall use of computer resources during the period shown in the figure were comparable to those of the Eta. The average grid distance of the Eta during the time considered was in fact about 7 km greater than that of the NGM over the contiguous United States, where the verification is performed. The Eta schemes are typically of the second-order accuracy, and none are higher than the second. Yet, the Eta displays a very considerable advantage over the NGM, across all of the categories monitored.

There are of course many differences between the two models which in one way or another contribute to the difference in precipitation scores. Different convection schemes may come to mind as the prime suspect. In this connection one should be reminded of tests made at the end of the eighties with the then Eta Model version of the Betts-Miller scheme, aimed at implementing

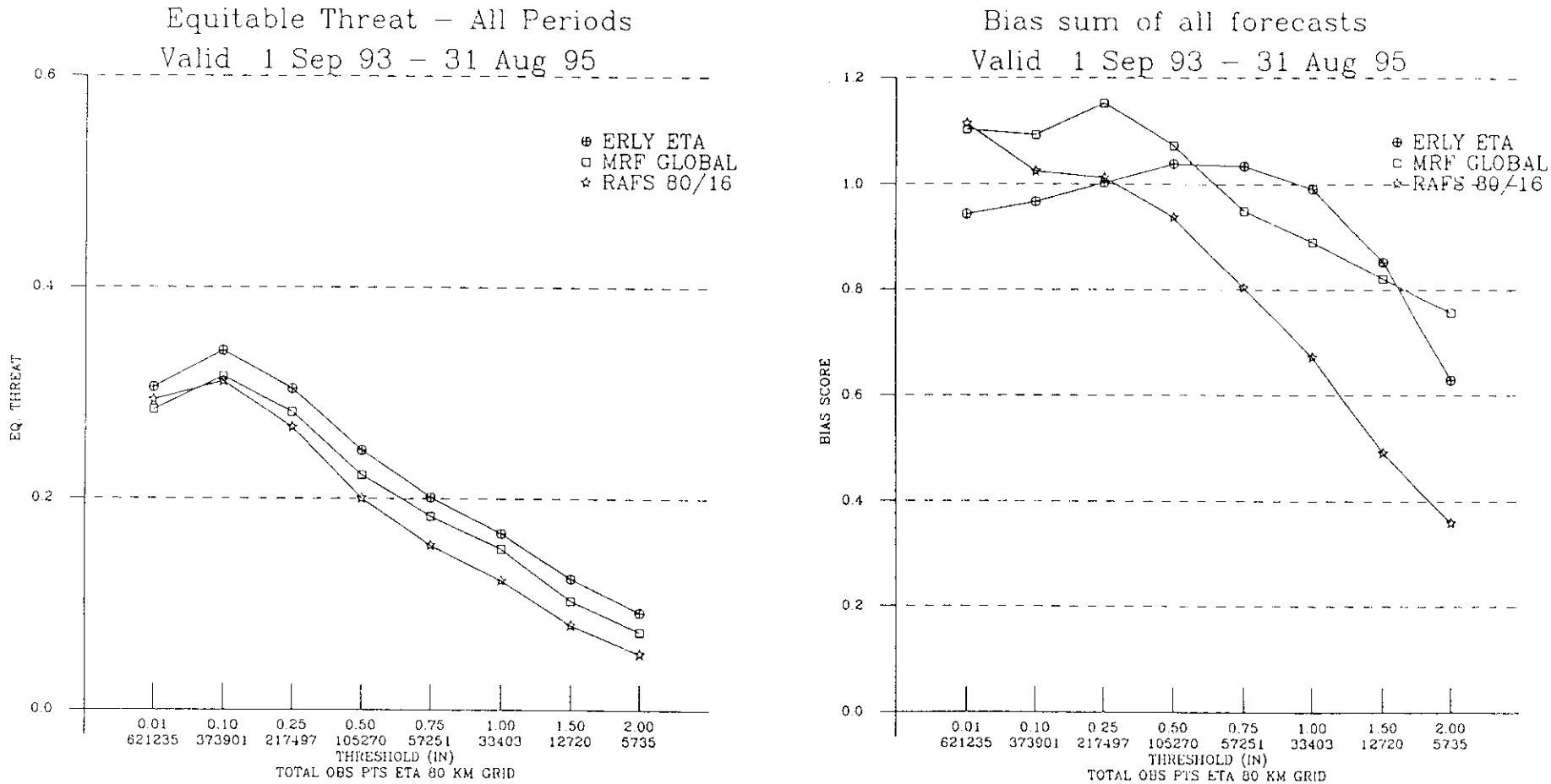

Fig. 7. Equitable precipitation threat scores (left panel) and bias scores (right panel), for the Eta 80-km Model (ERLY ETA), the Aviation/MRF Model (MRF GLOBAL) and NGM (RAFS), for the 24-month period September 1993-August 1995. The upper row of numbers along the two abscissas shows the precipitation thresholds, in inches/24 h and greater, which are verified. Scores are shown for a sample containing three verification periods, 0-24, 12-36, and 24-48 h. The sample contains 1,779 verifications by each of the three models.

the eta scheme in the NGM should that prove to be beneficial. While there were improvements for medium and particularly for heavier precipitation, threat scores at the lower categories became worse. Thus, the overall improvement was questionable and certainly not of the magnitude as to make the NGM's scores competitive with those of the Eta (Mesinger at al., 1990, Fig. 4; Plummer et al., 1989). Eventually the scheme was not implemented.

While the remaining components of the Eta's physics package of the period considered for the most part can be considered more advanced than those of the NGM, of the many sensitivity tests none have demonstrated impacts of the magnitude which would suggest physics to play a dominant role in the Eta vs NGM differences in forecast skill shown in Fig. 7. Regarding the initialization/assimilation systems of the two models, if anything, that of the NGM would be considered more advanced than that of the Eta prior to the implementation of EDAS in October 1995.

We are thus left with the difference in approaches to the numerical design of the two models as the prime candidate for the very considerable advantage in skill demonstrated by the Eta over the NGM during the period considered. It might perhaps be tempting to dismiss these results on account of the comparison not being a "clean" experiment. I do not believe we would be justified in disregarding this extremely large body of evidence. A tremendous amount of care and code checking has gone into the NGM and the likelihood of, for example, a major code error is extremely remote. The decision to "freeze" the model and discontinue its development has not been taken lightly. Thus, the advantage of the Eta over the NGM displayed in Fig. 7 I find a powerful indication of the advantage of the Arakawa over the "conventional" high-Taylor-series-accuracy, filtering-of-small-scales approach, for comprehensive atmospheric models of today. The qualification used here is motivated by the point already made in Section 2, of the forcing at individual model grid boxes by the physics packages in use. Such forcing is inconsistent with the high-formal-Taylor-series-accuracy concept, but is not in conflict with the fluid-dynamical considerations of the Arakawa approach to the design of numerical schemes, as outlined in the first two sections of the present paper.

6. Global modeling: The pole problem

A review paper with topics as covered so far would do no justice to the field without a reference to the pole problem of the Arakawa-like approach. Fourier filtering with the latitude-

longitude grid is not only obviously wasteful in terms of the excessive number of grid points carried in polar regions, but is also in conflict with the basic premise of the Arakawa approach of doing no artificial filtering at small scales at which the presumably important physical parameterizations are performed.

The purpose of this section is to emphasize the apparently very good prospects of constructing well-behaved global finite-difference models using the expanded cube approach, free of the two problems just mentioned. Pioneered by Sadourny (1972) again at a very early time, the idea has been reinvigorated recently by Rancic et al. (1996). Two different approaches they used for the shallow-water integrations to handle the line singularities of the expanded cube, both employing the Arakawa-type B/E grid Janjic (1977) momentum advection scheme, converged to a visually indistinguishable solution as the resolution was increased. The choice between the two approaches however was not clear, since the solution converging substantially faster, the one using a conformal grid, had a considerably less homogeneous distribution of points.

A still more recent extension of this work (Purser and Rancic, 1998) points a way to strike a balance between the two desirable features and relax the requirement of conformality to achieve a greater homogeneity, as might be found most cost-effective for the task at hand.

7. The Eta Model: The next 24 months, and the limited-area modeling concept.

With no proof of this being impossible, it is generally expected that through increased computing power and research and/or developmental work the skill of the operational prediction models should continue to improve. Indeed, various upgrades of the two "live" NCEP models/systems, the Eta and the Avn/MRF, have been taking place on a relatively regular basis during the time of and following the period of Fig. 7. For description of some of these upgrades see, e.g., Rogers et al. (1996), Chen et al. (1997), and Hong and Pan (1996). Specifically, the Eta upgrade of 12 October 1995 included an increase in horizontal resolution to about 48 km; for the impact of this upgrade during a six-month test period see Mesinger (1996b).

For an assessment of this hoped for improvement resulting from some of the implementations within the two systems, in Fig. 8 the equitable threat and bias scores for the 24-month period following that of Fig. 7 are shown. One should note that the Eta 48-km forecasts are for verification remapped to the previously used 80-km grid, in order not to penalize the higher

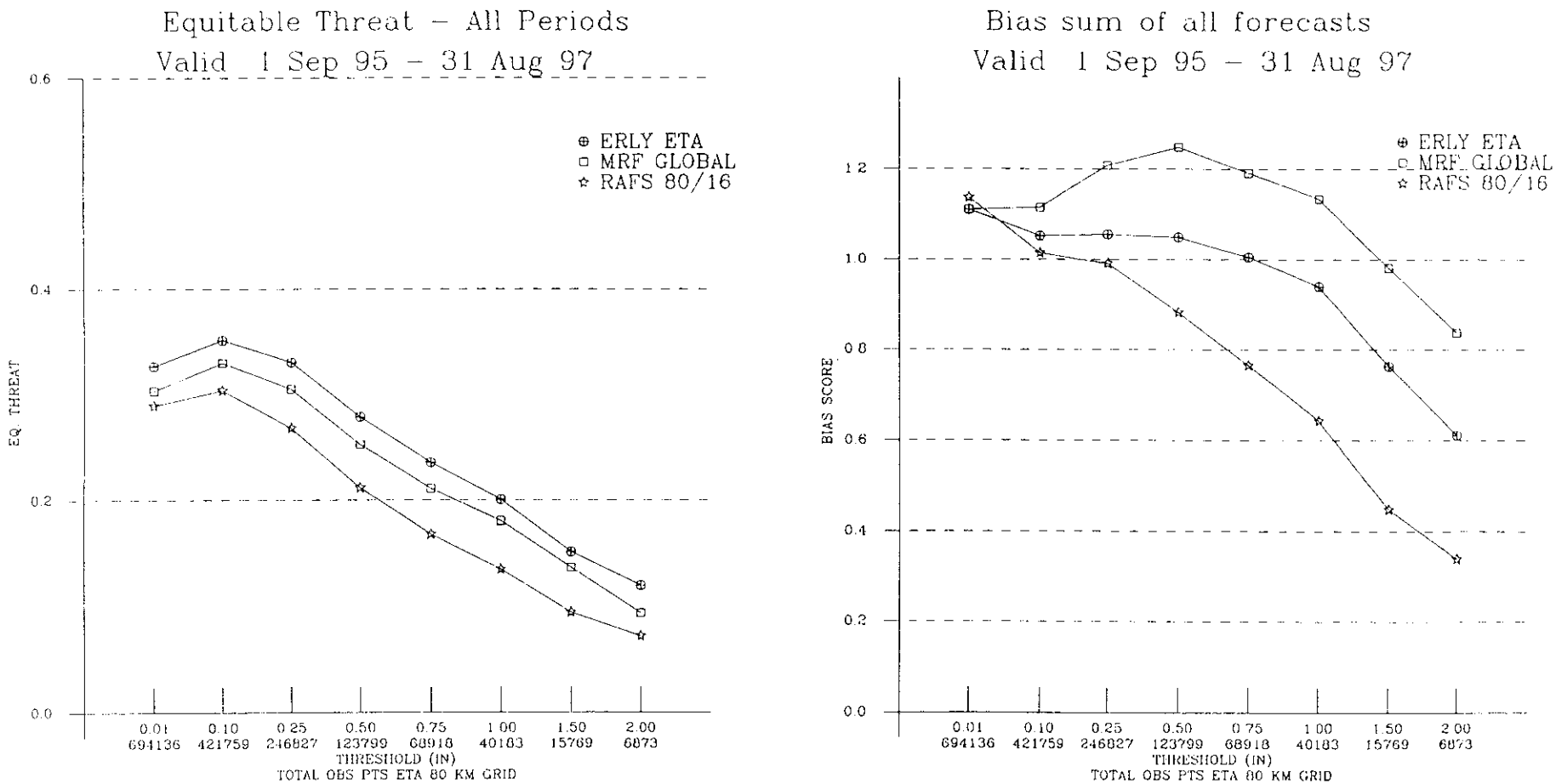

Fig. 8. Same as Fig. 7, except for the 24-month period September 1995-August 1997. The sample contains 1,970 verifications by each of the three models.

resolution model by the requirement to reproduce the increased noisiness of the 48-km box averages of the observed precipitation. Considerable improvement is indeed visible in the two live model threat scores relative to those of the frozen NGM. The scores of the NGM have of course also changed some, reflecting changes in the data which are entering the assimilation systems, and weather/climate variations between the two 24-month periods. Some weather events tend to result in higher scores than others, and in particular at the heaviest rain categories the impact of the frequency of occurrence in such scores-friendly events is noticeable. For example, more 80-km verification boxes with amounts of 2 inches and greater per verification period in the second 24 months than in the first, about 3.5 vs 3.2, is seen to be associated with increased threat not only of the two live models but of the NGM as well.

Once again, in Fig. 8 the Eta scores are significantly higher than those of its boundary condition driver Avn/MRF model. Compared to the preceding 24-month period, the difference between the two has in fact increased for most of the categories, at six out of the eight monitored.

One might wonder how does this advantage of the Eta depend on the forecast period, given that its lateral boundary conditions are 12-h old. One would expect that as the forecast progresses the older and thus less accurate lateral boundary information has more and more of an impact on the contiguous United States area, where the verification is performed, so that the Eta skill eventually starts lagging behind that of the Avn/MRF forecast of the same initial time.

For an assessment of the situation in this respect, in Fig. 9 threat scores for the same 24-month period of the 12-36 h forecasts, and of the 24-48 h forecasts are shown, in the left and the right panel, respectively. Inspection of the plots displayed reveals no obvious reduction in the advantage of the Eta over the Avn/MRF as the forecast period is increased from 12-36 to 24-48 h. In fact, at several of the categories in Fig. 9 the difference in threat scores between the Eta and the Avn/MRF is at 48 h greater than at 36 h. Clearly, the validity of the limited-area modeling concept, with the setup and models used here, is at 48 h not yet exhausted and a longer Eta run, provided the resources were available, would be justified.

This considerable advantage of the Eta over its driver model and in particular the resistance it displays to contamination by the advection of the apparently lower accuracy boundary condition, and/or contamination by the advection of the "lateral-boundary-condition-related difficulties" (Côté et al., 1998) into the domain of interest I find worthy of attention. Arguments have been raised at quite a number of places regarding the relative merits of the limited-area vs

the global variable-resolution strategy, in particular very recently by Côté et al. (1998). They summarize a considerable number of papers, ten to be precise, by stating that they "all indicate that lateral-boundary-condition error can, depending upon the meteorological situation, importantly contribute to the total error." They conclude by recommending that "more needs to be done to validate the methodologies employed by today's mesoscale models".

But especially in an operational setting, I find it difficult to imagine a more appropriate type of validation than the one presented here, of demonstrating the advantage the limited-area model achieves over its driver model. Note, in particular, this was done in spite of the imposed operational requirements that the limited-area forecasts be available *before* the driver model forecasts of the same initial time, and by using *less data*. It seems to me that this is the most rigorous "acid test", to adopt the term from Côté et al. (1998), and Yakimiw and Robert (1990), that "any successful limited-area model should meet", as this is the purpose the limited-area model has been set up for. This test may be contrasted with the one of the cited papers that "the solution obtained over a limited area should well match that of an equivalent-resolution model integrated over a much-larger domain". While demonstrating the latter is a most impressive task, of an obvious interest, it is hardly one having much of a practical meaning since were the integration of an equivalent-resolution model over a much-larger domain feasible, there would be no need to run a limited-area model in the first place. This is of course not meant to say that problems of the limited-area modeling are not most deserving of study. They in fact will continue to be addressed in the next section as well.

8. Limited area modeling: The resolution vs domain size trade-off

With the focus on numerical design, the question arises whether there are any specific features of the Eta numerics or setup that could be identified as making a notable contribution to its advantage as discussed in the preceding sections.

One feature on which clean tests have been made is that of the impact of the eta coordinate. They have been done using the switch of the model which permits the same code to be run as the eta and also as a sigma system model. The original test of this kind performed with a dry/minimum physics model revealed considerable noise when running the model using the sigma coordinate (Mesinger et al., 1988). This was interpreted as coming from sigma system errors. In a later study three cases were run, and a sample of nine consecutive forecasts (Mesinger and

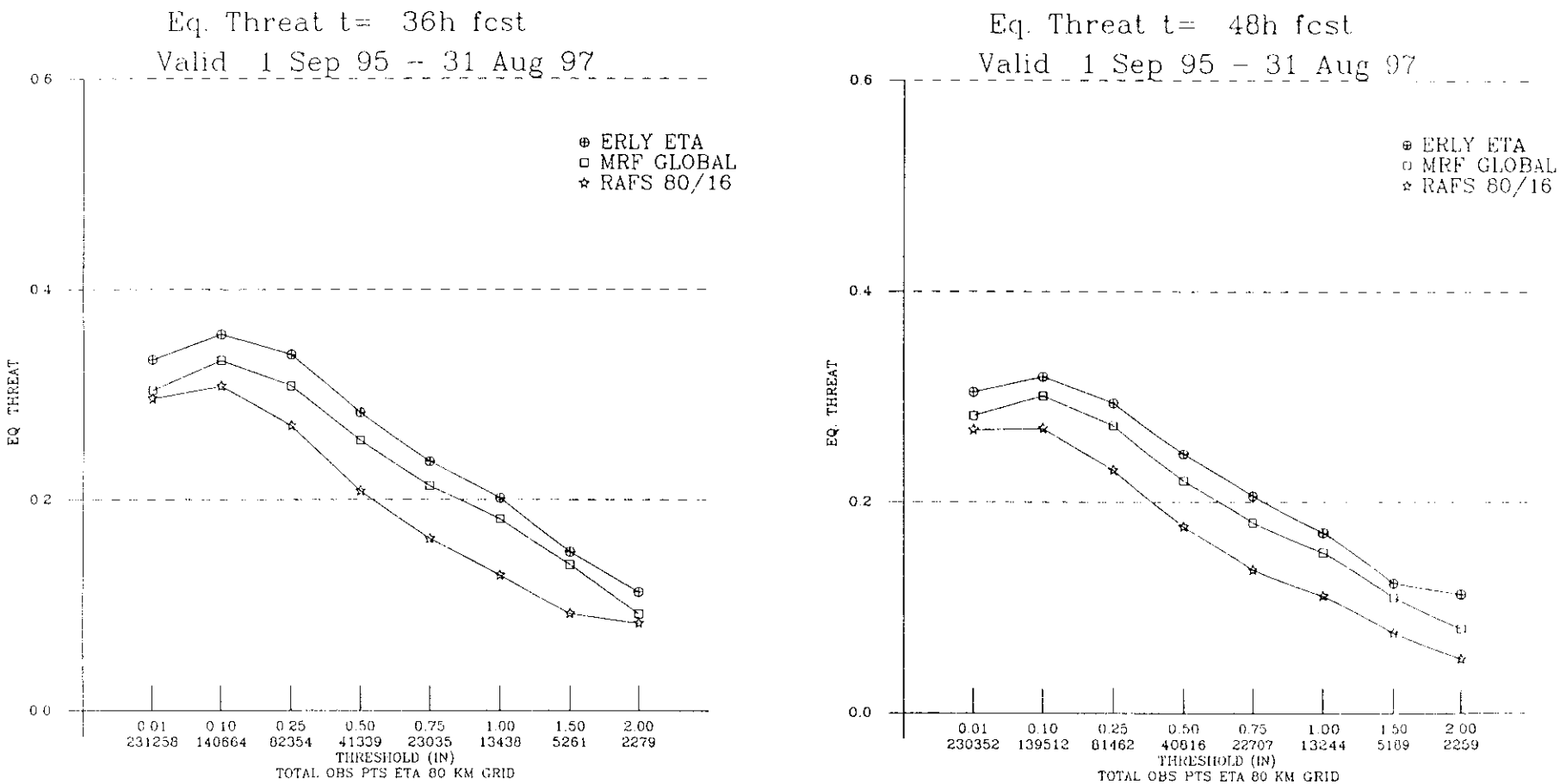

Fig. 9. Same as Fig. 8, except for verification periods of 12-36 h (left panel), and 24-48 h (right panel). Note that these are subsamples of the sample shown in Fig. 8. They contain 657 forecasts and 655 forecasts by each of the three models, for 12-36 and for 24-48 h verifications, respectively.

Black, 1992). This was followed by another study in which one case, and a sample of sixteen consecutive forecasts were run (Mesinger et al., 1997). In both samples the eta version of the model resulted in higher threat scores for all precipitation categories monitored. For more confidence in the model's sigma run it can be noted that in the second of the two samples the two other operational NCEP models were also included, with the Eta Model run as sigma winning convincingly all of the categories over the NGM, and winning by a wide margin most of the categories over the Avn/MRF model.

Results of three of the four individual cases mentioned above offered perhaps still more compelling evidence in favor of the eta coordinate, in the sense that the sigma runs of the Eta reproduced to a substantial degree errors of the two NCEP sigma system models, absent or for the most part absent in the Eta. Two of these errors are well documented as highly typical of the NCEP operational models: too slow southward propagation of cold surges east of the Rockies (Sullivan et al., 1993, Mesinger, 1996a), and placement of the lows as they form in the lee of the Rockies north of their analyzed positions (Mesinger et al., 1996).

Of these three cases, the three-model error statistics summarized in Mesinger et al. (1996) gives perhaps the most convincing evidence of the pervasiveness of the error. Of 15 lee lows within the sample considered which satisfied the rules set up, the Avn/MRF Model for example had placed all 15 north of their observed positions. The Eta, normally displaying little or no error of this kind, had reproduced the error when switched to sigma in one of the cases shown in Mesinger and Black (1992). Two more cases revealing the eta/sigma behavior of this kind are the arctic surge case of Mesinger and Black (1992), and the midtropospheric cutoff case of Mesinger et al. (1997).

Another Eta numerical design feature on which a considerable amount of statistics has been obtained is resolution. With the 80-km Eta, a test on the impact of the increase in vertical resolution from 17 to 38 layers has been made, running a sample of 148 forecasts (Mesinger et al., 1997). Three tests on the impact of the increase in horizontal resolution were made at various times (Black, 1994, Rogers et al., 1996, Mesinger et al., 1997), all from 80 to about 40 km, with 38 layers in the vertical. All of these tests have demonstrated a clear improvement resulting from increased resolution, in particular from that in the horizontal.

These results as well as evidence of numerous cases of improved simulations of orographically forced small-scale circulations (e.g., Black, 1994), along with practical

considerations, have led to operational implementation in 1995 of a higher-resolution version of the Eta. It was run and still is at the time of this writing at about 29 km horizontal resolution, and 50 layers in the vertical. I will refer to it as the "29-km Eta"; the name "Meso Eta" is also used. The operational setup of the 29-km Eta differs from the "Early Eta" in more ways than the resolution; there are altogether five differences between the two, as follows.

- 29 km/50 layers resolution, vs 48 km/38 layers of the Early Eta;
- 3:25 h data cutoff and use of this late cutoff for initializations at 0300 and 1500 UTC, vs the only 1:15 h cutoff of the Early Eta;
- "Current" vs 12-h old Avn lateral boundary conditions;
- A 3-h "mini" data assimilation vs the 12-h assimilation of the Early Eta; and
- Smaller domain size. The 48-km Eta domain is 106x80 deg, while the 29-km domain is 70x50 deg of rotated longitudexlatitude, respectively. Thus, the 29-km domain is by a factor of about 2.5 smaller than that of the 48-km Eta. The two domains are shown in Fig. 10.

The question naturally arises as to the impact of the differences between the two model setups on the model performance. Of the five differences listed, note that the first three would be expected to favor the 29-km model, and the last two the 48-km one. It would perhaps be generally expected that the first three should have by far a more dominant impact. Indeed, as stated, there are well-documented examples of benefits the 29-km Eta achieves, some of them clearly due to its better depiction of the local topography (e.g., Black, 1994; Schneider et al., 1996). Precipitation scores of the early period of the running of the model have appeared to support this expectation (Schneider et al., 1996).

With now more than two years of scores available, here in Fig. 11 threat and bias score plots of the two models for the 24-month period 16 October 1995 - 15 October 1997 are shown, along with those of the Avn/MRF model and of the NGM. The choice of mid-October 1995 for the starting time of this sample is made because of the already referred to upgrade of the Early Eta at that time. The sample contains 1,245 forecasts by each of the four models; 618 of them verifying at 24 h, and 627 verifying at 36 h. Note that the 29-km model is run only out to 36 h, or more precisely 33 h, so that these two verification periods only are available for all four of the models.

Inspection of the threat score plots displayed shows that the two Eta models exhibit a very

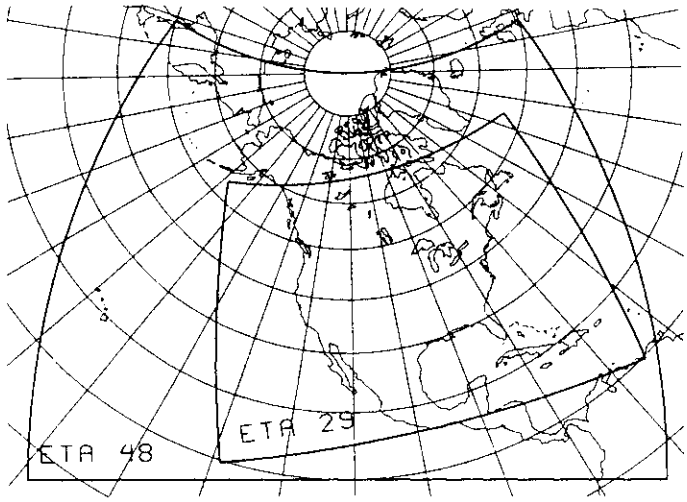

Fig. 10. The domains of the Eta 48-km and of the Eta 29-km model.

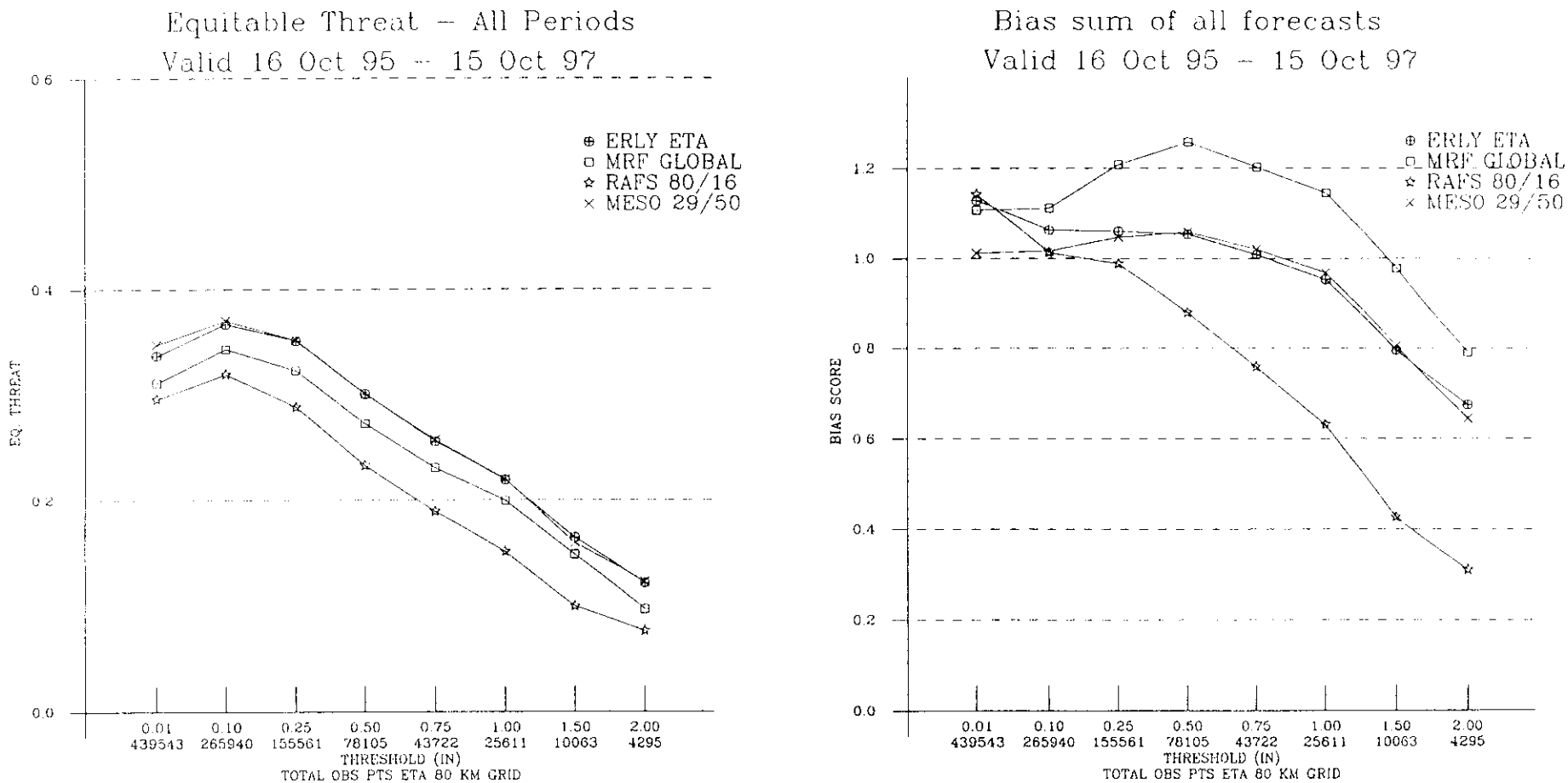

Fig. 11. Equitable precipitation threat scores for four of NCEP's operational models, those of preceding figures and for the "29-km Eta" (MESO), for various precipitation thresholds, and for the period 16 October 1995 - 15 October 1997, left panel; bias scores for the same models and period, right panel. "All Periods" refers to two verification periods, 00-24 h, and 12-36 h; note that the 29-km model is run only 33 h ahead. It is initialized 3 h later than the remaining models. The sample contains 1,245 forecasts by each of the four models; 618 of them verifying at 24 h, and 627 verifying at 36 h.

similar performance. The 29-km model is winning the two lowest categories, but it is losing the 1.5 inch category; the remaining categories are about a tie.

It would seem important to understand what could be the reason for this relatively successful performance of the 48-km model. The EMC precipitation forecast archiving system enables examination of scores for specific forecast and time periods. Given that the influence of the model's western boundary information should be felt more at 36 h than at 24 h, and that it could be expected to have more impact during winter than during the summer half of the year in view of stronger westerlies in winter, one might hope to detect some kind of a signal by subdividing the sample into 24 and 36 h forecasts and/or into "winter" and "summer" periods. Various subdivisions of this kind have been done and no clear signal was detected.

The relatively successful performance of the 48-km model thus remains somewhat of a puzzle. Recall, as referred to, that a clear benefit was obtained in clean resolution-only experiments when increasing the Eta resolution from 80 to 40 km, in three separate test periods.

A possible explanation is that performance of some of the model's parameterization schemes deteriorates when the resolution is increased beyond 40-50 km. This, of course, is a subject of attention but no obvious candidate problem has been identified.

Note however that for a given accuracy of the boundary conditions, and for a limited area model which for whatever reason intrinsically has more skill than its driver model, the domain size could help the performance of the limited area model by allowing it to develop larger scales of motion, consistent with the model and also more realistic than those of the driver model.

The evidence at hand, along with the lack of credible alternatives in view of the model differences and possibilities listed, thus suggests that the much larger domain size of the 48-km model is a significant and possibly the main contributor to its successful performance relative to that of the 29-km model.

9. Hurricane tracks

Still another indication of the benefits from emphasizing a large model domain of uniform resolution, and an Arakawa-style design, may be the Eta performance in forecasting tracks of major 1996 Atlantic hurricanes in comparison with that of models employing two competing concepts (Mesinger, 1998b). Successful Eta performance in forecasting tracks of various

hurricanes, tropical storms, or Pacific tropical cyclones was already noted early in the developmental work on the model (e.g., Kerr, 1990, Lazic, 1990, among others). Thus, Kerr (1990) refers to the experimental Eta's "uncommon hurricane prediction skill during the past season". More recent examples, of the Eta skill with the tracks of the 1995 hurricanes Allison and Felix, are described in Mesinger (1996b).

The statistics put together in Mesinger (1998b) seem worthy of note in connection with the issues raised in the preceding sections. For the two most intense landfalling Atlantic hurricanes of the 1996 season, Bertha and Fran, 48-h forecast position errors were compiled for the Eta 48-km and for three other NCEP operational models: the global (Avn) model, the regional spectral 50-km model (RSM, Juang et al., 1997), and the GFDL Hurricane Model (GHM, Kurihara et al., 1998). For Fran, errors of the Nested Grid Model (NGM) were also included in the comparison. NGM errors were not available for Bertha. For each storm, errors were compiled for six consecutive forecasts at 12 h intervals, the latest six forecasts having the hurricanes centered still over water at the initial time. In other words, of forecasts at 12-h intervals, in both cases the last six forecasts initialized before landfall were included.

The errors for both hurricanes are reproduced here in Table 1. The median and the average errors, for all 12 forecasts considered as one sample, are also displayed.

It should be stressed that what we are looking at are of course not differences only among models, but differences among forecasting systems including the data assimilation systems. In addition, the lateral boundary condition impact is involved in case of the Eta and the GHM, the Eta as stated before using the "old" and the GHM the "current" Avn boundary conditions. Note, in particular, that the Eta forecasts are available at approximately two and a half hours after the synoptic times of 0000 and 1200 UTC, as opposed to about 5 hours in case of the GHM.

Given the numbers of the table, an additional simple statistic is obtained by looking at how many times a model was the most accurate of the five. It is seen that the GHM and the Eta were each the most accurate three times, and have in addition shared the "first place" once; the RSM and the NGM were each the most accurate twice, and the Avn once. It is an instructive point to note that in a sample of only 12 forecasts, and five models of very different design including one at the time frozen for about five years, each of the models was best in at least one of the forecasts.

Regarding the overall performance, what is of interest here is the difference in approaches

TABLE 1. The NGM, Avn, RSM 50-km, Eta 48-km, and GHM 48-h errors, in km, in forecasting the position of Hurricane Bertha (July; NGM errors not available), and Hurricane Fran (September).

Verification time	NGM	Avn	RSM50	Eta48	GHM
0000 UTC 12 July	--	425	425	625	325
1200 UTC 12 July	--	900	750	300	250
0000 UTC 13 July	--	200	225	75	75
1200 UTC 13 July	--	175	100	125	150
0000 UTC 14 July	--	350	175	300	225
1200 UTC 14 July	--	550	475	475	450
1200 UTC 5 September	275	325	325	100	150
0000 UTC 6 September	350	525	500	100	250
1200 UTC 6 September	325	350	325	125	200
0000 UTC 7 September	75	575	500	200	150
1200 UTC 7 September	75	425	350	125	100
0000 UTC 8 September	100	75	150	125	200
Median Error	--	387.5	337.5	125	200
Average Error	--	405	360	225	210

between the Eta, the RSM, and the GHM. The Eta approach has been summarized already. The RSM is a nested spectral model, employing a perturbation approach to achieve higher resolution over the region of interest. GHM is a multiply nested grid point model, in 1996 run with two movable nests of 37 and 18.5 km resolutions. The resolution of its outside grid is 110 km. It is designed on a nonstaggered grid. As a dedicated hurricane model, it has an advanced vortex initialization scheme.

While the RSM is seen to result in some improvement over the Avn model, the improvement is not nearly of the magnitude to make it competitive with the Eta. Note that a comparison of the threat scores of the two models for 1996 (Mesinger, 1998a, Fig. 3) shows a significant advantage of the Eta, across all of the thresholds monitored.

Regarding the Eta vs the GHM, the relatively small size of the sample limits the significance of the results shown. Still, the fact that the GHM and the Eta are of a comparable accuracy in this sample raises questions relevant to modeling in general, and in particular the limited-area modeling. It suggests that there are components in the Eta system which compensate for the Eta disadvantages of using less data, using 12-h old lateral boundary conditions, having less horizontal resolution in the domain of the hurricane, and having no vortex initialization scheme -- if all of these indeed are advantages of the GHM compared to the Eta. To the extent they are, once again the uniform horizontal resolution over a very large model domain (and higher than the GHM coarse grid resolution) and also the staggered horizontal grid seem to me as the prime candidates which should come to mind.

The desirability of a large "pristine uniform-resolution" area, to adopt once more a term from Côté et al. (1998), is of course in conflict with the also very desirable increase in resolution. The experience summarized here I believe strongly points toward a careful cost/benefit analysis of the two, as opposed to succumbing to the intense lure of the high-visibility value of the resolution kilometer number. Note that in the framework of the 48- and the 29-km Eta versions discussed earlier, assuming a proportionate increase in the vertical resolution and various economies as practiced, a 1 km increase in horizontal resolution is equivalent to about a 10 % increase in the domain size. Thus, domain size is not expensive in terms of the benefits that it appears to offer.

10. The progress achieved

As background for information on the gain in the time validity of the precipitation forecasts, in Fig. 12 in the left panel equitable threat scores of 00-24 h forecasts of the Early Eta and of the NGM/RAFS are shown. Considerable gain in the accuracy of 24 h forecasts is seen achieved by the Eta over the NGM, going from close to 20 % in terms of the threat scores for low precipitation categories up to about a factor of 2 at the highest category monitored of 2 in/24 h and greater.

In the right panel of the figure the 24 h NGM threat score plot is reproduced along with that of the Early Eta 24-48 h forecasts. At the two ends the Eta scores are seen to be visibly higher, while for the intermediate categories the scores are very similar with a slight advantage overall in favor of the Eta as well.

Given that as stated (DiMego et al., 1992) the NGM has been frozen in August 1991, the right panel plot thus demonstrates that in terms of the official NMC/NCEP model-produced quantitative precipitation forecasts (QPF) in six years a gain in forecast validity of 24 h has been achieved. Put differently, for given accuracy, in six years the time validity of the NMC/NCEP model-produced QPF forecasts has doubled.

One should however note that this increase in the NMC/NCEP model QPF accuracy is the result of a cumulative impact of several effects, only one of which is the Eta model/system improvement during the six years. The two major remaining ones are the increased computing resources taken advantage of to increase the resolution as one change of the upgrade of October 1995; and the other the fact that the Eta QPFs were superior to those of the NGM already at the time the NGM was frozen. Note, for example the Eta's substantially higher threat scores across all of the categories of a sample of 58 forecasts of summer 1989, shown in the lower panel of Fig. 4 of Mesinger et al. (1990), with the two models using the same convection scheme.

11. Example of a successful forecast

To complement the considerable body of statistics summarized so far, in Fig. 13 a recent example of a successful precipitation forecast is shown. It is of a case of southern California heavy rains of early December 1997, affecting the symposium venue area as part of a pattern widely blamed on the intense El Niño of 1997/1998. In the upper panel the 48-km Eta forecast of 24-48 h accumulated precipitation, in inches, is shown. The amounts plotted are the 80-km box values as remapped for verification. In the lower panel the observed precipitation in mm/24

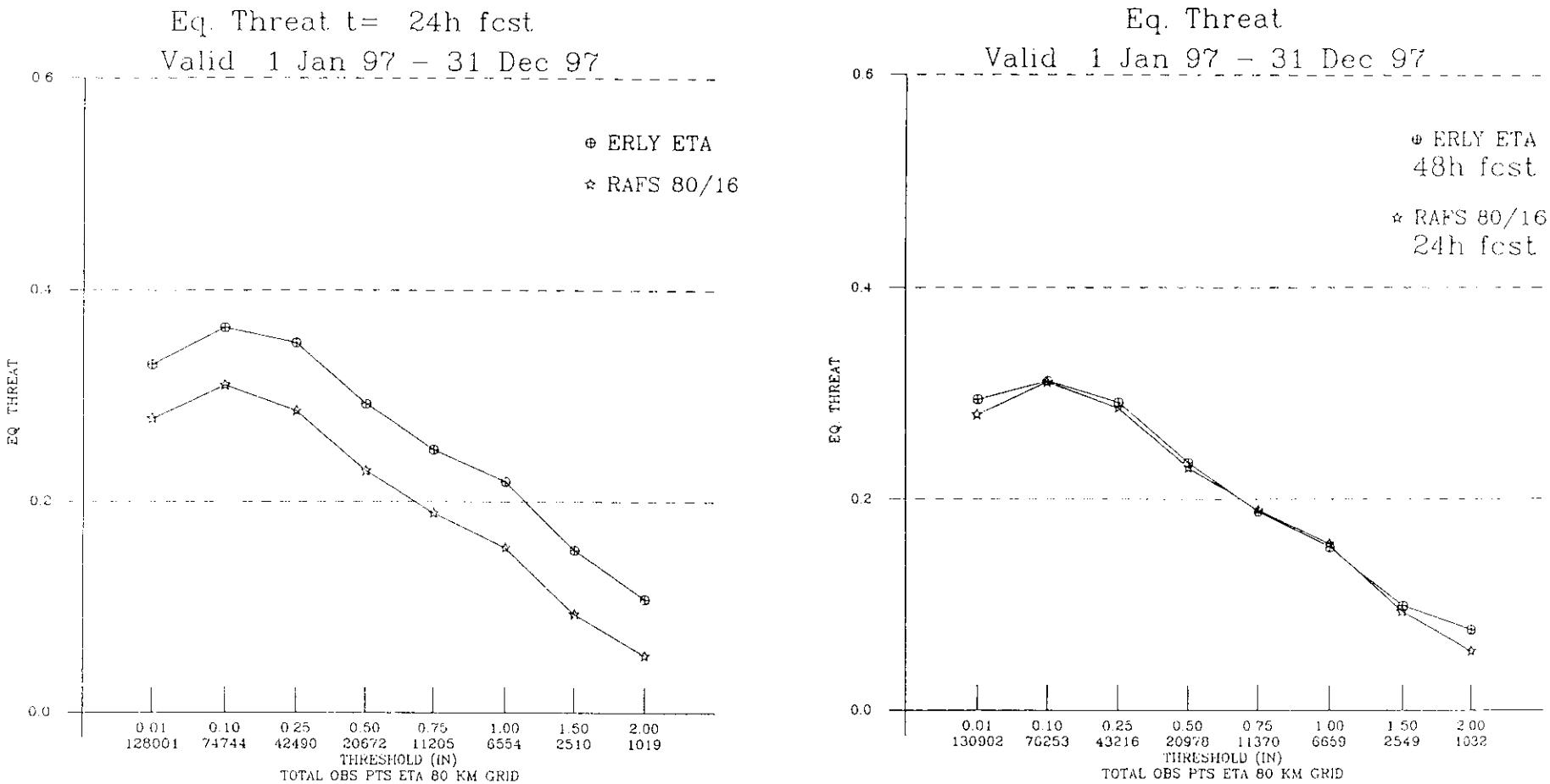

Fig. 12. Equitable precipitation threat scores of the Early Eta and of the NGM/RAFS for 00-24 h forecasts, left panel. The sample contains 348 verifications by each of the two models. Scores of the 24-48 h Early Eta shown against the 00-24 h NGM/RAFS scores, right panel.

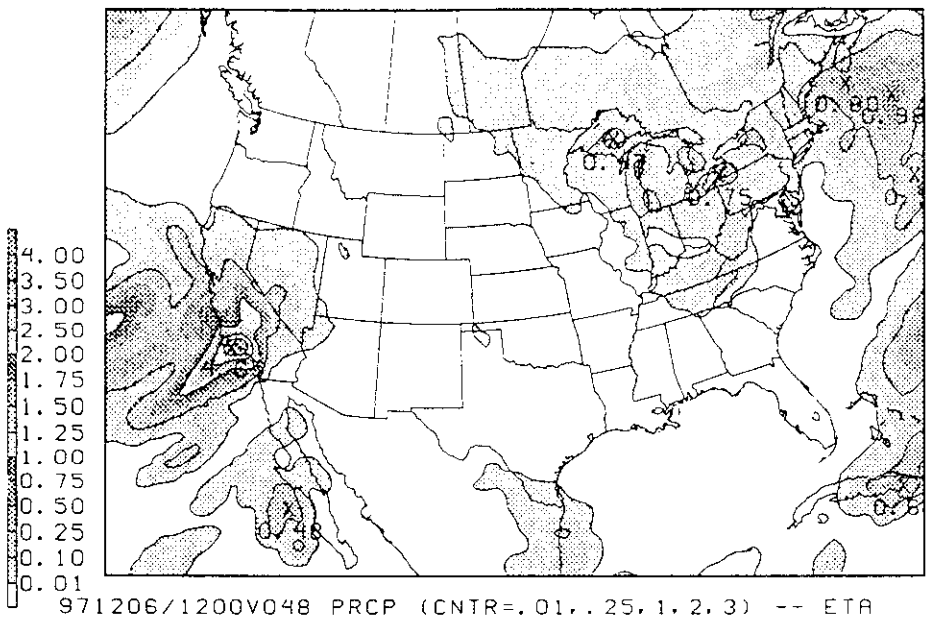

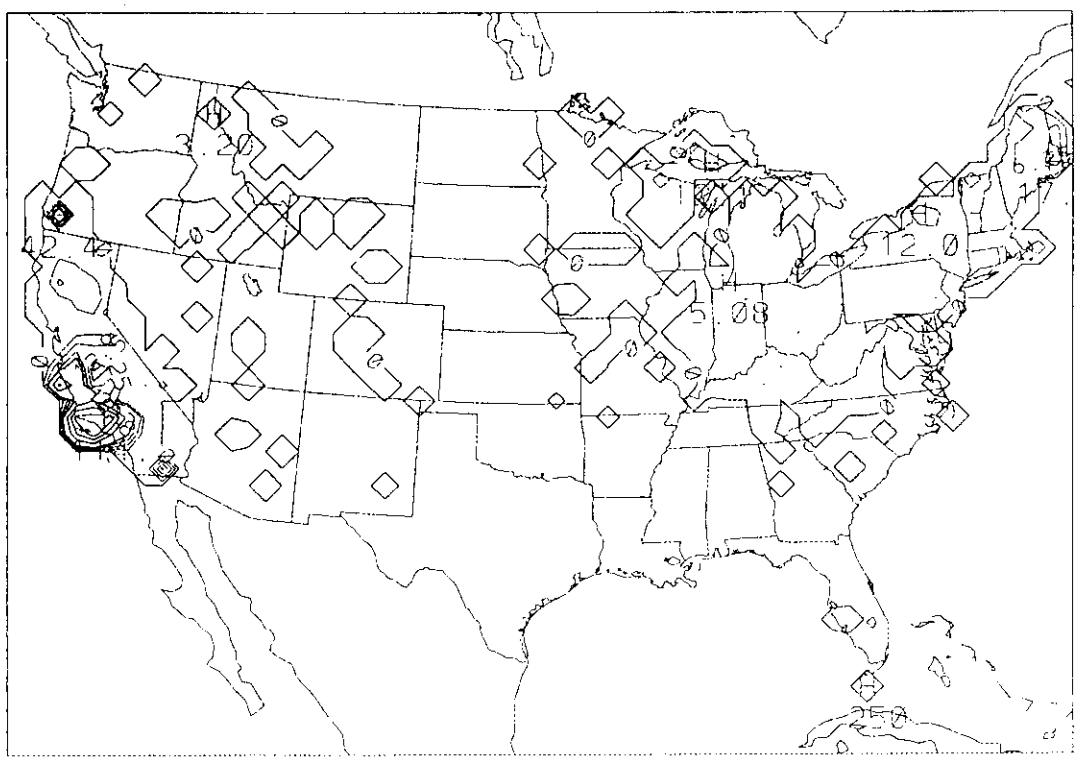

Fig. 13. The 48-km Eta forecast of 24-48 h accumulated precipitation, in inches,verifying 1200 UTC 6 December 1997, upper panel. EMC verification analysis of 24 h accumulated precipitation, in millimeters, verifying at the same time, lower panel. Both are values valid for 80-km boxes, remapped for the forecast, and averaged for the observed precipitation.

h is shown, also averaged over 80-km boxes.

The forecast maximum of 4.65 in/24 h is very close to the observed box maximum of 114 mm/24 h. The location of the forecast maximum is also well predicted, as was the one of the preceding 00-24 h forecast period over Florida (not shown). The verification analysis of the two 24 h periods resulted in 2 "points" (80-km boxes) of precipitation of 2 in and greater the first 24 h period, over Florida, and 6 points the second, over southern California. The model had forecast 1 point of 2 in and greater the first period, and 3 the second. All four forecast points verified. These were four "hits" out of a total of 114 that resulted in the Eta 24-48 h scores' advantage over the NGM's 00-24 h ones at 2 inches and greater that is seen in the right plot of Fig. 12.

12. Concluding remarks

The intention of the leading sections of this paper was to summarize some of the issues of the Arakawa approach in numerical methods, as an illustration of the variety of considerations that are made and opportunities which present themselves. This has also enabled me to review some of the recent ideas and results in addressing the horizontal grid problems. Propagation of gravity waves forced at individual grid points on a semi-staggered B/E grid was the central theme of this review.

The sections which followed for the most part contained a synopsis of the results of the Eta Model, viewed in comparison with other models of NMC, now NCEP. The Eta Model's early success in its mission of advancing the short-range forecasting skill over the contiguous United States I find strongly supportive of the benefits obtainable through an Arakawa-style numerical formulation used by the model, as opposed to a competing high-formal-accuracy, filtering-of-small-scales approach of the NGM.

These as well as some of the more recent Eta Model results summarized in later sections in addition seem to offer guidance regarding a number of central issues of the limited-area modeling strategy. One is that of the trade-off between the model resolution and domain size with indications of a considerable advantage the 48-km Eta is enjoying as a result of its uncommonly large "pristine uniform-resolution" (Côté et al., 1998) domain. Another is the related issue of the advection of lower-accuracy lateral boundary information with the Eta displaying a perhaps surprising degree of resilience to contamination by the 12-h old Avn lateral boundary data.

Large-sample comparisons of the typically second-order accurate Eta against the fourth-order NGM of the early period, and against the RSM with its spectral "infinite"-order accuracy in the horizontal at more recent times, are favorable to the Eta and bring once again into focus the issue of the numerical design priorities. While it has been stressed that the concept of the order of accuracy based on Taylor expansion "is not relevant" -- to adopt the expression of Arakawa (1997) -- regarding various issues addressed by the Arakawa approach, one might still wonder about reasons as to why the benefits of the higher formal accuracy which are typically very visible in simple test problems seem to be absent to such a degree in complex model integrations. Note, for example, the statement of Cullen et al. (1997) "use of the fourth order Heun [advection] scheme is essential to obtain results of this quality in the test problem. However, the sensitivity of the complete model to the choice between second and fourth order schemes at forecast resolutions (grid lengths less than 100 km) has been slight."

The forcing at individual model grid points done by physics packages of "complete" models is the obvious prime candidate answer. Recall that in physics the grid point values are treated as box averages. This assumes that box boundaries are treated as discontinuities. Of numerical schemes that have seen some application in meteorology perhaps the only one which treats grid point values as box averages allowing for possible discontinuities at box boundaries is the piecewise polynomial scheme, studied at some length by Carpenter et al. (1990). Enthusiasm seems lacking for a wider application of this approach because of the cost involved. Note however that various conservation constraints in the Arakawa style have no problem with the box-average interpretation of the grid point values, as this is precisely how the grid point values are treated in the difference analogs which are maintained.

Expectations are perhaps universal that further increases in resolution will result in significant further increase in weather prediction and climate simulation skill. This is based not only on the fact that smaller-scale terrain and other features will thereby be taken into account but also on encouraging results of actual integrations with higher resolution model versions. Regarding the Eta, note for example the report on the Eta 10-km effort by Black et al (1998). Many other examples could be cited, including also some from nonhydrostatic models run in a weather prediction mode.

Yet, I do not find that we should expect that the impact of the differences in numerical design should automatically diminish and eventually disappear as the resolution increases. Note that

the choices, if anything, are getting even more numerous due to the trend toward relaxation or removal of the hydrostatic assumption, and due to increasing computing power at our disposal. It is my expectation that, as a result, the rewards from judicious choices in the numerical design area, made with due regard to dynamical properties of the atmosphere/ocean, and physical parameterizations used, will only grow bigger.

Acknowledgments. Regarding the part of this paper summarizing the performance of the Eta Model, it is a pleasure to acknowledge that the development and implementation of a forecasting system, of which a model is only a part, results from dedicated work of many people. Only some of the contributors are mentioned in various references. The EMC's precipitation analysis and verification system was established originally by John Ward, with a contribution of the grid-to-grid remapping system by the present author; and has subsequently been further developed and is maintained now for many years by Mike Baldwin. Model's graphical archive resulting in plots such as the one of Fig. 13 and leading to numerous essential conclusions regarding the model performance has been established and is maintained by Keith Brill. Tom Black has read the manuscript and has provided many useful suggestions which have improved the quality of the text. Jim Purser has noted an error in the draft version of Fig. 3, upper panel; and along with Henry Juang, has provided other useful comments as part of the NCEP internal review of the manuscript.

On a more general level, the Eta Model research reported here would not have been possible without recourse to the extraordinary research environment of the Environmental Modeling Center and of other unique facilities at the U. S. National Centers for Environmental Prediction, Camp Springs, Maryland. In this sense and otherwise, support of Drs. Eugenia Kalnay, Director of the Center for most part of the period covered, Geoff DiMego, Chief of its Regional and Mesoscale Modeling Branch, and Ron McPherson, NCEP's Director, were vital.

References

Arakawa, A. (1966). Computational design for long-term numerical integration of equations of fluid motion: Two dimensional incompressible flow. Part I. J. Comput. Phys., 1, 119-143.

Arakawa, A. (1972). Design of the UCLA general circulation model. Numerical Simulation of Weather and Climate, Tech. Rep. 7, Department of Meteorology, University of California, Los Angeles, Los Angeles, CA, 116 pp.

Arakawa, A. (1988). Finite-difference methods in climate modeling. Physically-Based Modelling and Simulation of Climate and Climatic Change, Part I, M. E. Schlesinger, Ed., Kluwer, 79-168.

Arakawa, A. (1997). Adjustment mechanisms in atmospheric models. J. Meteor. Soc. Japan, 75, No. 1B, 155-179.

Arakawa, A., and V. R. Lamb (1977). Computational design of the basic dynamical processes of the UCLA general circulation model. Methods in Computational Physics, Vol. 17, J. Chang, Ed., Academic Press, 173-265.

Arakawa, A., and V. R. Lamb (1981). A potential enstrophy and energy conserving scheme for the shallow water equations. Mon. Wea. Rev., 109, 18-36.

Black, T. L. (1994). The new NMC mesoscale Eta Model: Description and Forecast Examples. Wea. Forecasting, 9, 265-278.

Black, T., M. Baldwin, G. DiMego, and E.Rogers (1998). Results from daily forecasts of the NCEP Eta-10 Model over the western United States. Preprints, 12th Conf. on Numerical Weather Prediction, Phoenix, AZ, Amer. Meteor. Soc., 246-247.

Black, T., D. Deaven, and G. DiMego (1993). The step-mountain eta coordinate model: 80 km 'Early' version and objective verifications. NWS Technical Procedures Bull. 412, National Oceanic and Atmospheric Administration/National Weather Service, 31 pp. [Available from National Weather Service, Office of Meteorology, 1325 East-West Highway, Silver Spring, MD 20910.]

Carpenter, R. L., Jr., K. K. Droegemeier, P. W. Woodward, and C. E. Hane (1990). Application of the piecewise parabolic method (PPM) to meteorological modeling. Mon. Wea. Rev., 118, 586-612.

Chen, F., Z. Janjic, and K. Mitchell (1997). Impact of atmospheric surface-layer parameterizations in the new land-surface scheme of the NCEP mesoscale Eta Model. Bound.-Layer Meteor., 85, 391-421.

Côté, J., S. Gravel, A Méthot, A. Patoine, M. Roch, and A. Staniforth (1998). The operational CMC-MRB Global Environmental Multiscale (GEM) Model. Part I: Design considerations and formulation. Mon. Wea. Rev., 126, (in press).

Cullen, M. J. P., T. Davies, M. H. Mawson, J. A. James, and S. C. Coulter, (1997). An overview of numerical methods for the next generation UK. NWP and climate model. Numerical Methods in Atmospheric and Oceanic Modelling, C. Lin, R. Laprise, and H. Ritchie, Eds. The André J. Robert Memorial Volume. Canadian Meteorological and Oceanographic Society/NRC Research Press. 425-444.

DiMego, G. J. (1988). The National Meteorological Center regional analysis system. Mon. Wea. Rev., 116, 977-1000.

DiMego, G. J., K. E Mitchell, R. A. Petersen, J. E. Hoke, J. P. Gerrity, J. J. Tuccillo, R. L. Wobus and H.-M. H. Juang (1992). Changes to NMC's regional analysis and forecast system. Wea. Forecasting, 7, 185-198.

Heikes, R., and D. A. Randall (1995a). Numerical integration of the shallow-water equations on a twisted icosahedral grid. Part I: Basic design and results of tests. Mon. Wea. Rev. 123, 1862-1880.

Heikes, R., and D. A. Randall (1995b). Numerical integration of the shallow-water equations on a twisted icosahedral grid. Part II: A detailed description of the grid and an analysis of numerical accuracy. Mon. Wea. Rev. 123, 1881-1887.

Hollingsworth, A., P. Källberg, V. Renner, and D. M. Burridge (1983). An internal symmetric computational instability. Quart. J. Roy. Meteor. Soc., 109, 417-428.

Hong., S.-Y., and H.-L. Pan (1996). Nonlocal boundary layer vertical diffusion in a medium-range

forecast model. Mon. Wea. Rev., 124, 2322-2339.

Janjic, Z. I. (1977). Pressure gradient force and advection scheme used for forecasting with steep and small scale topography. Contributions to Atmospheric Physics, 50, 186-199.

Janjic, Z. I. (1979). Forward-backward scheme modified to prevent two-grid-interval noise and its application in sigma coordinate models. Contrib. Atmos. Phys., 52, 69-84.

Janjic, Z. I. (1984). Nonlinear advection schemes and energy cascade on semi-staggered grids. Mon. Wea. Rev., 112, 1234-1245.

Janjic, Z. I. (1994). The step-mountain eta coordinate model: Further developments of the convection, viscous sublayer, and turbulence closure schemes. Mon. Wea. Rev., 122, 927-945.

Janjic, Z. I. (1996a). The Mellor-Yamada level 2.5 scheme in the NCEP Eta Model. Preprints, 11th Conf. on Numerical Weather Prediction, Norfolk, VA, Amer. Meteor. Soc., 333-334.

Janjic, Z. I. (1996b). The surface layer in the NCEP Eta Model. Preprints, 11th Conf. on Numerical Weather Prediction, Norfolk, VA, Amer. Meteor. Soc., 354-355.

Janjic, Z. I., T. L. Black, and G. DiMego (1998). Contributions toward development of a future community mesoscale model (WRF). Preprints, 16th Conf. on Weather Analysis and Forecasting, Phoenix, AZ, Amer. Meteor. Soc., 258-261.

Janjic, Z. I., and F. Mesinger (1984). Finite difference methods for the shallow water equations on various horizontal grids. Numerical Methods for Weather Prediction. Seminar 1983, ECMWF, Shinfield Park, Reading, U.K., 29-101.

Janjic, Z. I., and F. Mesinger (1989). Response to small-scale forcing on two staggered grids used in finite-difference models of the atmosphere. Quart. J. Roy. Meteor. Soc., 115, 1167-1176.

Janjic, Z. I., F. Mesinger, and T. L. Black (1995). The pressure advection term and additive splitting in split-explicit models. Quart. J. Roy. Meteor. Soc., 121, 953-957.

Ji, Y., and A. D. Vernekar (1997). Simulation of the Asian summer monsoons of 1987 and 1988 with a regional model nested in a global GCM. J. Climate, 10, 1965-1979.

Juang, H.-M. H., and J. E. Hoke (1992). Application of fourth-order finite differencing to the NMC Nested Grid Model. Mon. Wea. Rev., 120, 1767-1782.

Juang, H.-M. H., S.-Y. Hong, and M. Kanamitsu (1997). The NCEP regional spectral model: An update. Bull. Amer. Meteor. Soc., 78, 2125-2143.

Kanamitsu, M., J. C. Alpert, K. A. Campana, P. M. Caplan, D. G. Deaven, M. Iredell, B. Katz, H.-L. Pan, J. Sela, and G. H. White (1991). Recent changes implemented into the global forecast system at NMC. Wea. Forecasting, 6, 425-435.

Kerr, R. A. (1990). Hurricane forecasting shows promise. Science, 247, 917.

Kurihara, Y., R. E. Tuleya, and M. A. Bender (1998). The GFDL hurricane prediction system and its performance in the 1995 hurricane season. Mon. Wea. Rev., 126, (in press).

Lazic L. (1990). Forecasts of AMEX tropical cyclones with a step-mountain model. Austr. Meteor. Mag., 38, 207-216.

Leslie, L. M., and R. J. Purser (1991). High-order numerics in an unstaggered three-dimensional time-split semi-Lagrangian forecast model. Mon. Wea. Rev., 119, 1612-1623.

McDonald, A (1997). Lateral boundary conditions for operational regional forecast models; a review. HIRLAM Tech. Rep. 32, 32 pp. [Available from A. McDonald, Irish Meteorological Service,

Glasnevin Hill, Dublin 9, Ireland.]

Mesinger, F. (1973). A method for construction of second-order accuracy difference schemes permitting no false two-grid-interval wave in the height field. Tellus, 25, 444-458.

Mesinger, F. (1974). An economical explicit scheme which inherently prevents the false two-grid-interval wave in the forecast fields. Proc. Symp. Difference and Spectral Methods for Atmosphere and Ocean Dynamics Problems, Academy of Sciences, Novosibirsk 1973; Part II, 18-34.

Mesinger, F. (1977). Forward-backward scheme, and its use in a limited area model. Contrib. Atmos. Phys., 50, 200-210.

Mesinger, F. (1982). On the convergence and error problems of the calculation of the pressure gradient force in sigma coordinate models. Geophys. Astrophys. Fluid. Dyn., 19, 105-117.

Mesinger, F. (1984). A blocking technique for representation of mountains in atmospheric models. Riv. Meteor. Aeronautica, 44, 195-202.

Mesinger, F. (1993). Forecasting upper tropospheric turbulence within the framework of the Mellor-Yamada 2.5 closure. Res. Activities Atmos. Oceanic Modelling, Rep. 18, WMO, Geneva, 4.28-4.29.

Mesinger, F. (1996a). Forecasting cold surges east of the Rocky Mountains. Preprints, 11th Conf. on Numerical Weather Prediction, Norfolk, VA, Amer. Meteor. Soc., 68-69.

Mesinger, F. (1996b). Improvements in quantitative precipitation forecasts with the Eta regional Model at the National Centers for Environmental Prediction). The 48-km upgrade. Bull. Amer. Meteor. Soc., 77, 2637-2649; Corrigendum, 78, 506.

Mesinger, F. (1998a). Quantitative precipitation forecasts of the "early" Eta Model: An update. Preprints, 16th Conf. on Weather Analysis and Forecasting, Phoenix, AZ, Amer. Meteor. Soc., 184-186.

Mesinger, F. (1998b). Performance of the 48-km Eta in forecasting tracks of major landfalling Atlantic hurricanes of the 1966 season, Bertha and Fran. Preprints, 16th Conf. on Weather Analysis and Forecasting, Symp. on the Research Foci of the U.S. Weather Research Program, Phoenix, AZ, Amer. Meteor. Soc., 526-528.

Mesinger, F., and A. Arakawa (1976). Numerical Methods used in Atmospheric Models. WMO, GARP Publ. Ser. 17, Vol. I, 64 pp. [Available from World Meteorological Organization, Case Postale No. 5, CH-1211 Geneva 20, Switzerland.]

Mesinger, F., and T. L. Black (1992). On the impact on forecast accuracy of the step-mountain (eta) vs. sigma coordinate. Meteor. Atmos. Phys., 50, 47-60.

Mesinger, F., T. L. Black, and M. E. Baldwin (1997). Impact of resolution and of the eta coordinate on skill of the Eta Model precipitation forecasts. Numerical Methods in Atmospheric and Oceanic Modelling. C. Lin, R. Laprise, and H. Ritchie, Eds. The André J. Robert Memorial Volume. Canadian Meteorological and Oceanographic Society/NRC Research Press. 399-423.

Mesinger, F., T. L. Black, D. W. Plummer and J. H. Ward (1990). Eta model precipitation forecasts for a period including Tropical Storm Allison. Wea. Forecasting, 5, 483-493.

Mesinger, F., and Z. I. Janjic (1974). Noise due to time-dependent boundary conditions in limited area models. The GARP Programme on Numerical Experimentation, Rep. 4, WMO, Geneva, 31-32.

Mesinger, F., and Z. I. Janjic (1985). Problems and numerical methods of the incorporation of mountains in atmospheric models. Large-scale Computations in Fluid Mechanics, Part 2. Lect. Appl. Math., 22, Amer. Math. Soc., 81-120.

Mesinger, F., Z. I. Janjic, S. Nickovic, D. Gavrilov, and D. G. Deaven (1988). The step-mountain coordinate: Model description and performance for cases of Alpine lee cyclogenesis and for a case of an Appalachian redevelopment. Mon. Wea. Rev., 116, 1493-1518.

Mesinger, F., R. L. Wobus, and M. E. Baldwin (1996). Parameterization of form drag in the Eta Model at the National Centers for Environmental Prediction. Preprints, 11th Conf. on Numerical Weather Prediction, Norfolk, VA, Amer. Meteor. Soc., 324-326.

Nickovic, S. (1994). On the use of hexagonal grids for simulation of atmospheric processes. Contrib. Atmos. Phys., 67, 103-107.

Oliger, J., and A. Sundström (1978). Theoretical and practical aspects of some initial boundary value problems in fluid dynamics. SIAM J. Appl. Math., 35, 419-446.

Pan, H.-L., and W.-S. Wu (1994). Implementing a mass-flux convective parametrization package for the NMC Medium-Range Forecast Model. Tenth Conf. on Numerical Weather Prediction, Portland, OR, Amer. Meteor. Soc., 96-98.

Plummer, D. W., T. L. Black, N. A. Phillips, and J. E. Hoke (1989). Tests of the Betts-Miller convective parameterization in the Nested Grid Model. Research Highlights of the NMC Development Division: 1987-1988. NOAA/NWS, 23-25. [Available from the NOAA Environmental Modeling Center, 5200 Auth Road, Camp Springs, MD 20746.]

Popovic, J. M., S. Nickovic, and M. B. Gavrilov (1996). Frequency of quasi-geostrophic modes on hexagonal grids. Meteor. Atmos. Phys., 58, 41-49.

Purser, R. J., and M. Rancic (1998). Smooth quasi-homogeneous gridding of the sphere. Quart. J. Roy. Meteor. Soc., 124, 637-647.

Rancic, M., R. J. Purser, and F. Mesinger (1996). A global shallow-water model using an expanded spherical cube: Gnomonic versus conformal coordinates. Quart. J. Roy. Meteor. Soc., 122, 959-982.

Randall, D. A. (1994). Geostrophic adjustment and the finite-difference shallow-water equations. Mon. Wea. Rev., 122, 1371-1377.

Rogers, E., D. G. Deaven, and G. J. DiMego (1995). The regional analysis system for the operational "early" Eta Model. Wea. Forecasting, 10, 810-825.

Rogers, E., T. L. Black, D. G. Deaven, G. J. DiMego, Q. Zhao, M. Baldwin, N. W. Junker, and Y. Lin (1996). Changes to the Operational "Early" Eta Analysis/Forecast System at the National Centers for Environmental Prediction. Wea. Forecasting, 11, 319-413.

Sadourny, R. (1972). Conservative finite-differencing approximations of the primitive equations on quasi-uniform spherical grids. Mon. Wea. Rev., 100, 136-144.

Sadourny, R., and P. Morel (1969). A finite-difference approximation of the primitive equations for a hexagonal grid on a plane. Mon. Wea. Rev., 97, 439-445.

Schneider, R. S., and Coauthors (1996). The performance of the 29 km Meso Eta model in support of forecasting at the Hydrometeorological Prediction Center. Preprints, 11th Conf. on Numerical Weather Prediction, Norfolk, VA, Amer. Meteor. Soc., J111-J114.

Thacker, W. C. (1978). Comparison of finite-element and finite-difference schemes. Part II: Two-dimensional gravity-wave motion. J. Phys. Oceanogr., 8, 680-689.

Yakimiw, E., and A. Robert (1990). Validation experiments for a nested grid-point regional forecast model. Atmos.-Ocean, 28, 466-472.

Williamson, D. (1969). Integration of the barotropic vorticity equation on a spherical geodesic grid.

Mon. Wea. Rev. 97, 512-520

Winninghoff, F. J. (1968). On the adjustment toward a geostrophic balance in a simple primitive equation model with application to the problems of initialization and objective analysis. Ph. D. Thesis, Dept. Meteor. Univ. California, Los Angeles, CA 90024.

Zhao, Q., and F. H. Carr (1997). A prognostic cloud scheme for operational NWP models. Mon. Wea. Rev., 125, 1931-1953.